University of South-Eastern Norway

www.usn.no

FMH606 Master's Thesis 2023
Process Technology

Design and construction of a bubbling fluidized bed reactor with two side nozzles as inlet flow boundary condition

Suraj Shrestha

Faculty of Technology, Natural Sciences, and Maritime Sciences
Campus Porsgrunn

University of South-Eastern Norway

www.usn.no

Course: FMH606 Master's Thesis, 2023

Title: Design and construction of a bubbling fluidized bed reactor with two side nozzles as inlet flow boundary conditions

Number of pages: 61

Keywords: Fluidized bed reactor, nozzle, distributor plate, minimum fluidization, mixing and segregation, pressure drop, superficial velocity, density, CPFD, bubbles, sand particles, biomass particles

Student:	Suraj Shrestha
Supervisor:	Prof. Rajan Kumar Thapa, Rajan Jaiswal
External partner:	Dr. Abdul Rahim Nihmiya

University of South-Eastern Norway

www.usn.no

Summary:
Fluidized bed reactors are commonly used in industrial applications such as waste to energy conversion, chemical synthesis, granulation, catalyst regeneration, biomass gasification, pyrolysis, etc. They are used in such applications due to their efficient mixing, uniform heat, and mass transfer and better temperature control. Gas distribution inside the reactor plays a crucial role in determining the conversion process and fluidization regime. The air distributor plate is the most common method of gas distribution. However, it has drawbacks such as increased auxiliary power requirements and frequent cleaning and maintenance due to clogging of pores by sintering and small particles. As an alternative, fluidizing the particle bed with a nozzle helps overcome air distribution problems.

This study focuses on the construction of bubbling fluidized bed reactor with two side nozzles as inlet flow boundary conditions. The results of the bubbling fluidized reactor with side nozzles are compared with the bubbling fluidized bed reactor with distributor plate. This is done by studying the flow behavior of binary mixtures of Geldart B and Geldart D particles through a series of experiments. A Computational Particle Fluid Dynamics (CPFD) model was developed using EMMS-Yang-2004 drag models in Barracuda Software and validated using experimental data.

The results indicate that the reactor with two side nozzles has lower fluidization velocity than the reactor with distributor plate. The results also show that as the percentage of biomass increases in both reactors the minimum fluidization velocity decreases. In both reactors, good mixing of biomass and sand particles was observed after fluidization, and segregation of binary mixture was observed at a higher superficial gas velocity. Good mixing of binary mixture decreased on increasing biomass percentage in sand particles. Biomass segregates from the middle part of reactor with side nozzles whereas particles segregate from the bottom end of the reactor with uniform distribution. Mostly larger Bubbles were seen from the sides of the reactor after fluidization in the reactor with side nozzles. However, smaller bubbles were seen all over the reactor bed with the distributor plate reactor.

Preface

The thesis “Design and construction of a bubbling fluidized bed reactor with two side nozzles as inlet flow boundary conditions," is part of a master’s degree program at the University of South-Eastern Norway, Porsgrunn. This thesis explores the benefits of using nozzles rather than distributor plates for fluidizing gas supply in fluidized bed reactors. The project involves both experimental and simulation tasks, aimed at characterizing the fluid dynamics behavior of the reactors.

Writing my thesis was an exciting experience that taught me to think creatively and critically. I'm grateful to Supervisor Rajan Kumar Thapa for helping me during my master's program, and to Co-Supervisor Rajan Jaiswal for his continuous support. I also appreciate the contributions of Dr. Abdul Rahim Nihmiya, (Senior Lecture, Dept. of Civil and Environmental Technology, University of Sri Jayewardenepur) an external partner who helped me make sense of my research findings.

Porsgrunn, 08/05/2023

Suraj Shrestha

Contents

Nomenclature

Symbol	Descriptions	SI Unit
U_{mf}	Minimum fluidization velocity	m/s
d_p, d_m	Mean particle size	m
U_{mb}	Minimum bubbling velocity	m/s
U_c	Critical velocity	m/s
$\varepsilon_m, \varepsilon_{mf}$	Void fraction in a fixed bed, in a bed at minimum fluidization condition	-
ΔP_b	Pressure drops per across bed	Pascal
A_t	Cross section area of the bed	m^2
ρ_g, ρ_s	Gas density, density of solid	kg/m^3
g_c, g	Conversion factor, acceleration due to gravity	$\left[\frac{9.8\ kg.m}{kg-w.s^2}\right], m/s^2$
μ	Viscosity of gas	$kg/m.s$
$\emptyset_s$	Sphericity of particle	-
Ar	Archimedes Number	-
Re_p	Particle Reynolds number	-
φ	ratio of observed bubble flow	-
u_b, u_0	Bubble rise velocity, superficial gas velocity	m/s
Q_b	Rate at which bubble volume passes	m^3/s
h	Height of bed	m
h_{mf}	Height of minimum fluidization	m

ε_b	Bubble fraction	-
d_b	Effective bubble diameter	m
U_f, U_p	Lower gas velocity, Upper gas velocity	m/s
ρ_b, ρ_p	Bulk density, density of particle	kg/m^3
Q_{cp}	Ratio of bulk and particle density	-

LIST OF FIGURES

LIST OF TABLES

1 Introduction

1.1 Background

Fluidized bed reactors are used in various industrial process like chemical synthesis, granulation, drying of pharmaceutical products and raw agricultural products, chemical looping, biomass gasification and pyrolysis[1]. Different applications require different fluidized bed flow regimes, and the kind of flow regime that can be accomplished depends on several factors, such as superficial gas velocity, particle properties, and bed dimensions. Based on these factors, numerous studies have looked at fluidized beds' characteristics[2]. The distribution of gas inside fluidized bed reactors has a significant impact on their efficiency. This is due to the fact that the distribution of gas throughout the bed has a significant impact on both the conversion process and the operating fluidization regime of the reactor.[3]. An illustration for this, when biomass or waste is converted into gas using a bubbling fluidized bed reactor, the feedstock is transformed into gases with a higher calorific value. This process occurs in the presence of a limited amount of oxidizing agent. The success of the conversion process depends on the distribution of the fluidizing gas throughout the reactor cross-section, which determines the amount of oxidizing medium present for the feedstock conversion.[4]

The movement of bubbles rising within the particle bed, which is governed by numerous bubble parameters such as their rise velocity, diameter, and frequency, affects how particles behave in a reactor. Moreover, the distribution of gas, specifically the fluidizing gas, within the reactor has an impact on the mixing of larger biomass particles with the bed material as well as the reactor's overall operating regime. Through a distributor or nozzles, this fluidizing gas may be injected into the particle bed[5].

First, the construction of a bubbling fluidized bed reactor with two side nozzles as inlet flow boundary conditions is the first step to the thesis's goal. Then other objective of this research is to investigate the fluid dynamics behavior of the reactor. This is done by conducting experiments with the bed material of a binary mixture of Geldart B and Geldart D particles.

A series of experiments was carried out on both reactor, reactor with distributor plate and reactor with side nozzles as inlet flow boundary conditions. This was done to compare the results of both reactor and determine the flow regimes, which include the minimum fluidization, mixing and segregation, bubble dynamics, solid volume fractions, etc. to accomplish this goal. Additionally, a Computational Particle Fluid Dynamic (CPFD) model was developed to validate the experimental data and to predict the flow behavior of the hot bed conditions with side nozzles as flow boundary conditions.

1.2 Objective

The aim of this work is to optimize the hydrodynamic behavior of a fluidized bed reactor by using two sides of nozzles instead of a distributor plate for the gas supply. To achieve that goal, the following objectives were accomplished.

- ✓ Literature review on bubbling fluidized bed reactor, hydrodynamic behaviour of cold model bubbling fluidized bed reactor.
- ✓ Develop a bubbling fluidizing bed reactor model with two side nozzles instead of distributor plates.
- ✓ Identify the character of fluidizing behaviour in term of minimum fluidization, mixing and segregation properties by conducting series of experiments with binary particle of Geldart B and Geldart D particle.
- ✓ Identify and compare of fluidization regimes of both reactor one with distributor plate and another with two side nozzles as inlet boundary conditions through experiments.
- ✓ Developing Computational Particle Fluid Dynamics Models (CPFD) of reactor and validate with experimental data.
- ✓ Predict the flow behavior of the hot bed conditions with side nozzles as flow boundary conditions.

1.3 Overview of thesis

The structure of this report is as follows: An overview of the task background, objective and thesis overview of the report are provided in Chapter 1. Chapter 2 covers the literature survey, along with an overview of fluidized bed reactors, fluidization regimes and techniques for distributing gas. Chapter 3 explains Material and Methods selection. The research approach, including the design and construction of bubbling fluidizing bed reactor with two side nozzles as inlet boundary conditions, Equipment, Procedure, and experimental setup are described in detail in Chapter 4. Chapter 5 describes the simulation setup. Chapter 6 analyzes and discusses the results and findings of experiments and simulations. The conclusion of the entire work of presented results is discussed in Chapter 7.

2 Literature review

2.1 Fluidization

When a gas is moved through a group of loosely packed solid particles in an upward direction, they exhibit the fluid like behavior known as fluidization. The solid particles expand and vibrate when a gas is introduced into the column containing them by a gas distributor, counteracting the drag force the gas stream exerts on them[6]. Depending on the inlet gas properties (superficial gas velocity), bed qualities (material density, shape, and size), and bed dimensions, the fluidized bed exhibits characteristics similar to those of a dynamic liquid state and can range from a loose bed to pneumatic conveyance[7]. A clearly defined flow regime is crucial for fluidized bed chemical conversion[8]. When the gas velocity is raised above the bed's minimum fluidization velocity, a bed may switch from one regime to another. Particulate, bubbling, slugging, turbulent, rapid, and pneumatic conveyance regimes are among the fluidized bed regimes[9].

2.2 Fluidization Regimes

The behavior of a fluidized bed containing solid particles depends on factors such as the velocity of the gas flowing through it, the properties of the solid particles, and the characteristics of the gas. Different fluidization regimes can be observed in a fluidized bed, as illustrated in Figure 2.1.

When a fluid is passed through a fine particle bed at a low flow rate, the fluid moves through the empty spaces between the particles, creating a fixed bed as shown in Figure 2.1a. Then as the flow rate increases, the particles start to move and vibrate, which spreads out them and forms an expanded bed. The pressure drop across the bed eventually equals the weight of the fluid and particles in the section and the flow rate eventually reaches a point where all the particles are suspended by the fluid. This is known as minimum fluidization and is represented in figure 2.1b with a minimum fluidization velocity, U_{mf}.

When the flow rate exceeds the minimum fluidization rate, the bed expands smoothly creating a homogeneously fluidized bed as shown in Figure 2.1c. However, this type of bed is only observed under specific circumstances with small, light particles and dense gas at high pressure. Further increasing the flow rate results instabilities with bubbling and gas channeling occur. This type of bed is called a bubbling fluidized bed, as shown in Figure 2.1d. Bubbles in a bubbling fluidized bed coalesce and grow, and if the height to bed diameter ratio is high enough, the bubbles may reach almost the bed's diameter, causing slugging as in Figure 2.1e. For coarse particles, the portion of the bed above the bubble experiences a piston-like force, which eventually causes the slug to break apart and fall apart. The oscillatory action is repeated when a new slug begins to form. Figure 2.1f displays a flat slug.

If the gas flow rate is high enough, the particles in a fluidized bed can move faster than their terminal velocity. This causes a turbulent motion of diverse sized and shaped solid clusters and gas voids. This is called a turbulent bed, as shown in Figure 2.1E. If the gas velocity keeps increasing, the fluidized bed turns into an entrained bed where particles are sparsely scattered in the gas stream, which is similar to pneumatic solid transport.[10].

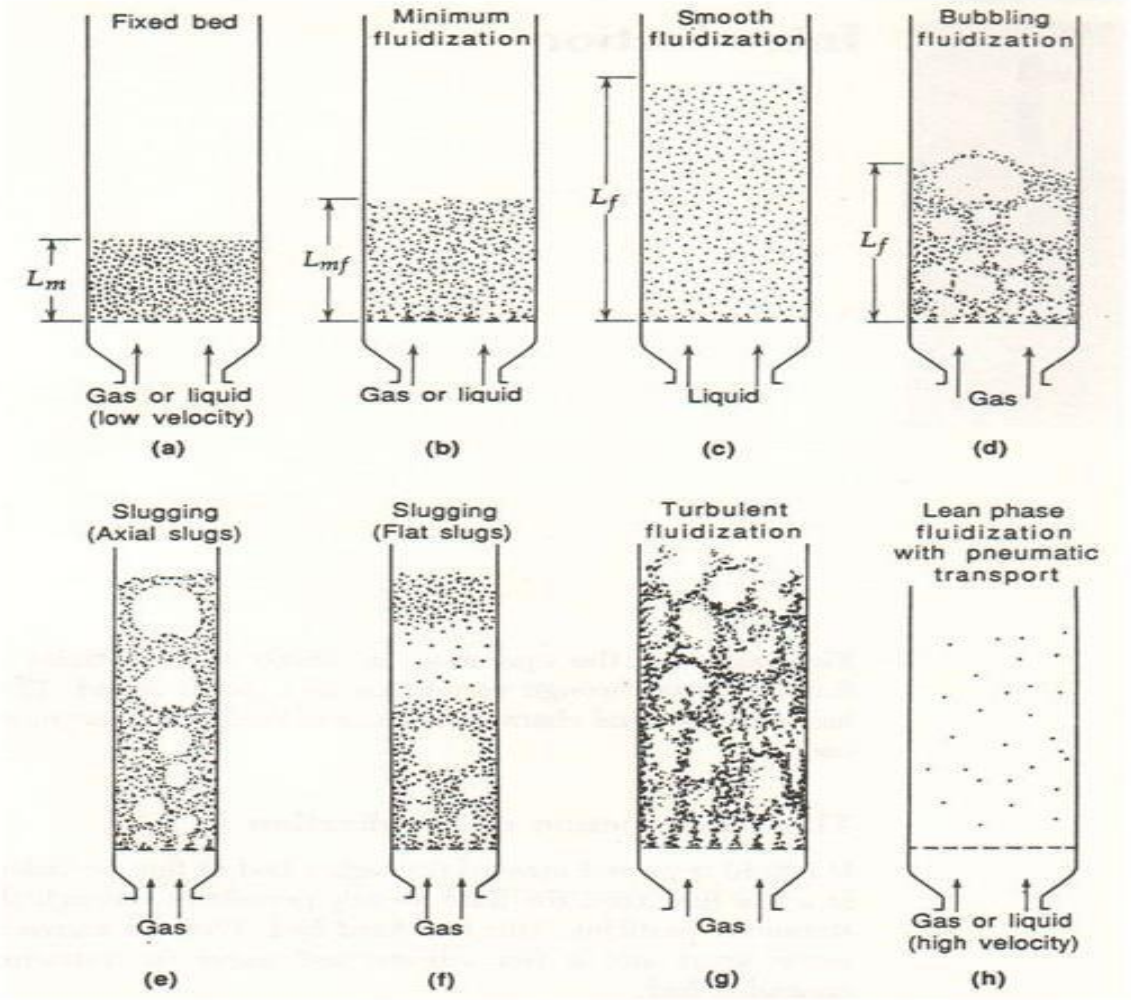

Figure 2.1 Schematic diagram of Fluidized bed of different regimes[10].

2.3 Geldart's classification of powder

Solid particles' size and density have the biggest impact on how they behave in fluidized beds. Figure 2.2 illustrates a detailed observation by Geldart (1973, 1978), who defined the properties of the four main powder types as follows:

- The characteristics of Group A particles, known as "aeratable" particles, include low particle density (1.4 g/cm^3) and small mean particle sizes (d_p 30 μm), making them easy to fluidize and rapid bubbles appears at the velocity higher than minimum bubbling velocity U_{mb}.

- Group B particles are referred to as "sand like" particles and typically range in size from 150 μm to 500 μm, with densities between 1.4 and 4 g/cm^3. When the minimum fluidization velocity is surpassed for these particles, the excess gas takes the form of bubbles, which can grow to a large size in a bed of Group B particles. Glass beads and coarse sand are two examples of frequently used Group B materials.

- Group C materials are Cohesive or fine powders with sizes smaller than 30 μm, making them difficult to fluidize due to strong interparticle forces. They are prone to channeling in small diameter beds. Examples include talc, flour, and starch.

-
- Group D materials which are referred to as "spoutable," are difficult to fluidize in deep beds because they are very big or very dense. When the gas distribution is unequal, they display significant channeling and spouting behavior. Examples include roasted metal ores, lead shot, and coffee beans [11].

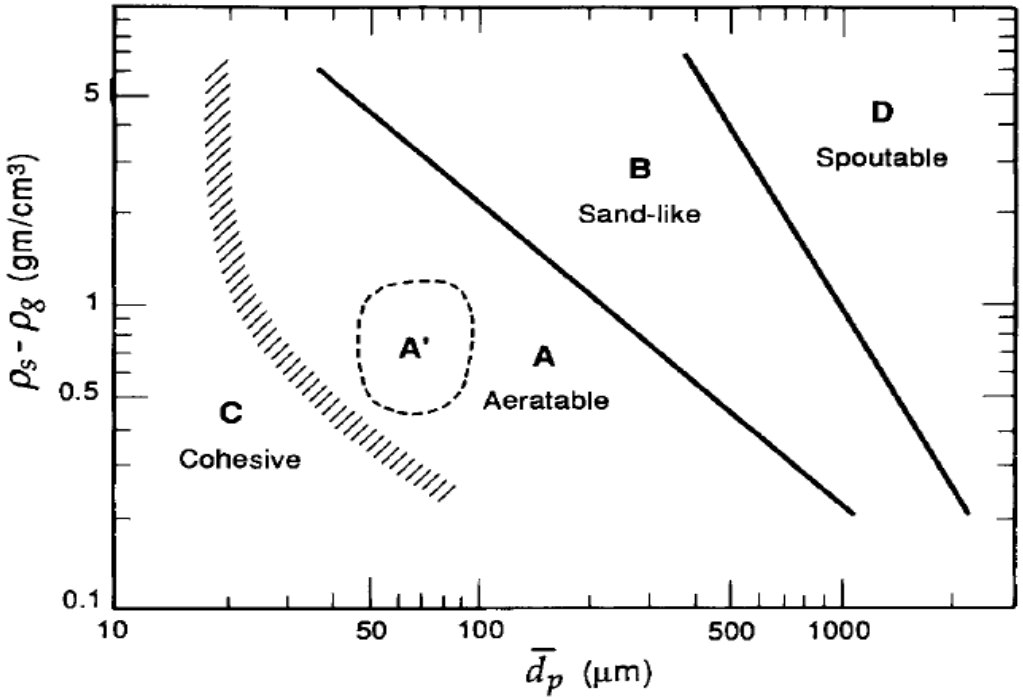

Figure 2.2 Geldart classification of particles for air at ambient conditions[12]

2.4 Bubbling fluidized bed

The movement of particles in fluidized beds is mainly influenced by the fluidization velocity, bubbles behaviors, bubbles path through bed etc. which are therefore carefully studied. To depict the actions taking place inside a fluidized bed reactor, the fluidization principles, bubble formation and these important parameters are explained below[11].

2.4.1 Minimum Fluidization velocity

The fluid velocity needed to simply suspend a bed's particles in a reactor and start the fluidization process is known as the minimum fluidization velocity. At this velocity, the bed expands, and the particles start to move randomly, which reduces the bed pressure drop. Any additional increase in fluid velocity causes the void fraction and bed pressure drop to rise[13].

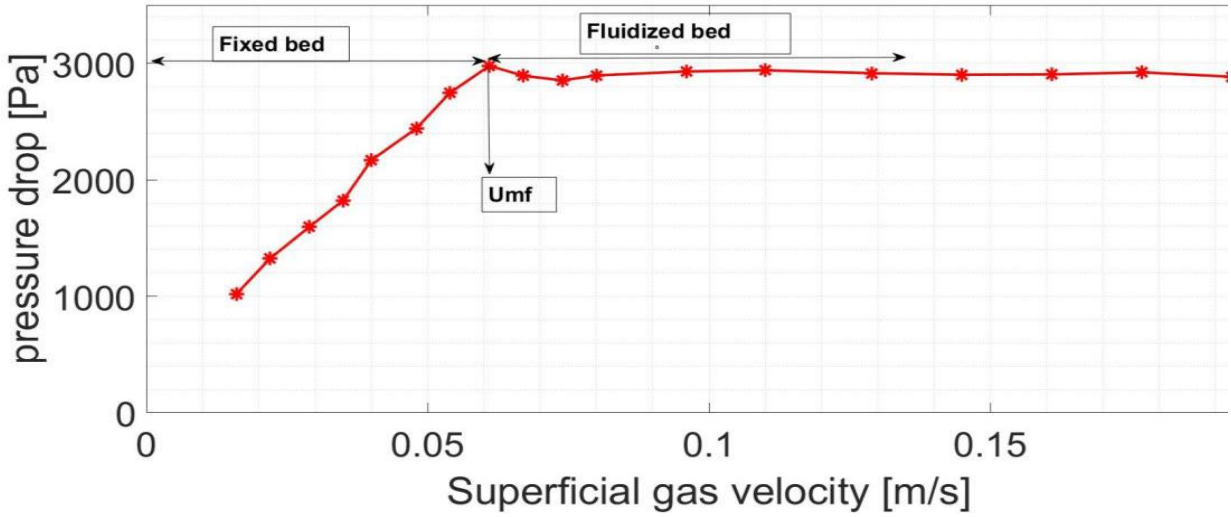

Figure 2.3 Pressure drop vs superficial gas velocity of a sand particle of 234.7 micron[7]

The onset of fluidization occurs when,
$\{pressure\ drop\ across\ bed\}\ \{cross\ sectional\ area\ of\ tube\} = \{volume\ of\ bed\}\ \{fraction\ consisting\ of\ solids\}\ \{specific\ weight\ of\ solids\}$
or, with Δp is always positive,

$$\Delta p_b A_t = A_t L_{mf}(1 - \varepsilon_{mf})\left[(\rho_s - \rho_g)\frac{g}{g_c}\right] \tag{2.1}$$

$$\frac{\Delta p_b}{L_{mf}} = (1 - \varepsilon_{mf})\left[(\rho_s - \rho_g)\frac{g}{g_c}\right] \tag{2.2}$$

Where g_c is conversion factor $\left[\frac{9.8\ kg.m}{kg-w.s^2}\right]$
Ergun[14] provides the frictional pressure drop across the bed for isotropic solids.

$$\frac{\Delta p_{fr}}{L_m} g_c = \frac{150(1-\varepsilon_m)^2}{\varepsilon_m^3}\frac{\mu\mu_0}{(\emptyset_s d_p)^2} + \frac{1.75(1-\varepsilon_m)}{\varepsilon_m^3}\frac{\rho_g \mu_0^2}{\emptyset_s d_p} \tag{2.3}$$

$$\frac{1.75}{\varepsilon_{mf}^3 \emptyset_s}\left(\frac{d_p u_{mf}\rho_g}{\mu}\right)^2 + 150\frac{150(1-\varepsilon_{mf})}{\varepsilon_{mf}^3 \emptyset_s^2}\left(\frac{d_p u_{mf}\rho_g}{\mu}\right) = \frac{d_p^3 \rho_g(\rho_s - \rho_g)g}{\mu^2} \tag{2.4}$$

$$\frac{1.75}{\varepsilon_{mf}^3 \emptyset_s} Re_{p,mf}^2 + \frac{150(1-\varepsilon_{mf})}{\varepsilon_{mf}^3 \emptyset_s^2} Re_{p,mf} = Ar \tag{2.4}$$

$$Ar = \frac{d_p^3 \rho_g(\rho_s - \rho_g)g}{\mu^2} \tag{2.5}$$

2.4.2 Bubble size and bubble rise velocity

Some of the most important fluidized bed dynamic properties that are crucial to the design of gas-solid fluidized bed reactors include bubble size, shape, and rise velocity. To determine the bubble shape and bubble rise velocity in a fluidized bed, various models have been developed. If gas velocity is increased beyond the minimum fluidization, then the bubbles is started to form in bed which term as bubble gas. As an expression, the bubble gas velocity is:

$$u_b = \Psi A_t(u_0 - u_{mf}) \quad (2.6)$$

Where Ψ is ratio of observed bubbles flow to that expected from two phase theory,
A_t is cross section area of bed,
u_b is velocity of bubble rise through bed,
u_0 is superficial gas velocity.

For Geldart A, B and D particles, Hilligardt and Werther[15] proposed Ψ for ${}^{z}/_{d_t} \cong 1$, as 0.8, 0.65 and 0.26. Moreover, Werther[16] provided bubble rise velocity that considers the full range of Geldart particle types and vessel size.

$$u_b = \Psi A_t(u_0 - u_{mf}) + a u_{br} \quad (2.7)$$

Then,

Geldart-type particle	A	B	D
a	$3.2d_t^{\frac{1}{3}}$	$2d_t^{\frac{1}{2}}$	0.87
d_t (m)	0.05-1.0	0.1-1.0	0.1-1.0

u_{br} may be determined from the bubble rise velocities in the Davidson and Harrison[17] model:
For a single bubbles:

$$u_{br} = 0.711(gd_b)^{0.5} \quad (2.8)$$

Like this, Werther [16] suggests the following equation for bubble size at any height z in a bed of Geldart particle B:

$$d_b(cm) = 0.853\left[1 + 0.272\left(u_0 - u_{mf}\right)\right]^{1/3} + (1 + 0.684z)^{1.21} \quad (2.9)$$

Conditions

$d_t > 20cm$ $\quad 1 \leq u_{mf} \leq 8cm/s$

$100 \leq d_p < 350\mu m$ $\quad 5 \leq u_0 - u_{mf} \leq 30cm/s$

2.4.3 Flow Pattern of Fluidization Bubbles

Bubbles rise from the bed and merge to form bigger bubbles. When these bubbles grow too large, they divide into smaller ones, as shown in Figure 2.4. The type of particles present influences when the bubbles in the bed reach their equilibrium size. Group A particles have a relatively small maximum stable diameter. As a result, the average size of bubbles stabilizes near the distributor plate and stays the same throughout the entire bed. For the case of Group B particles, it has a maximum stable diameter which is larger, and the point of equilibrium is generally achieved only in the upper regions of the bed. But in case of the behavior of bubbles in group D particle beds is distinct, as they do not ascend individually but instead move in swarms horizontally associated with each other. [11].

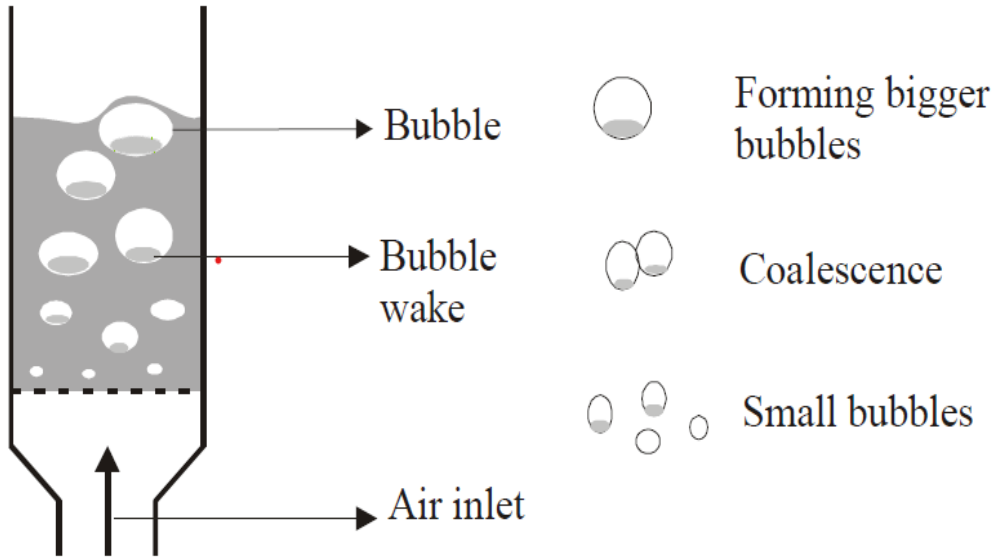

Figure 2.4 A freely bubbling fluidized bed and bubble coalescence modes[11].

2.4.4 Bed Expansion

The average fraction of the bed area occupied by bubbles can be calculated using an average bubble velocity, $< U_b >$ as follows:

$$\varepsilon_b = \frac{Q_b}{A_{bed}.< U_b >} \quad (2.10)$$

By assuming that the particulate phase's void fraction is equal to the void fraction at minimum fluidization and that all gas more than that amount flows through the bed as bubbles, the height h of the bed can be determined by

$$h - h_{mf} = \int_0^h \frac{Q_b}{A_{bed}. < U_b >} dz \tag{2.11}$$

If the bubble velocity is constant across the bed, the bed height can be determined by

$$\frac{h - h_{mf}}{h_{mf}} = \frac{U - U_{mf}}{U_b} \tag{2.12}$$

The proportion of the bed that is made up of bubbles is then equal to the bed's expansion:

$$\varepsilon_b = \frac{h - h_{mf}}{h} \tag{2.13}$$

The bubble fraction generally differs slightly from this theoretical value. <C2>[11].

2.5 Particle Mixing and Segregation

A binary mixture of solids' mixing index measures the degree of homogeneity between the two particles based on their percentage composition. Values range from 0, which is regarded as a condition of perfect segregation, to 1, which is referred to as perfect mixing. An equilibrium particle distribution that fluctuates with height in the bed results from simultaneous mixing and segregation by rising bubble motion[20]. A binary mixture of particles segregates when the drag per unit weight of the particles differs significantly. The particles travel upward when the drag per unit weight is strong, while they tend to sink to the bottom when the drag per unit weight is low[21].

2.5.1 Theoretical analysis for binary mixture

In the fluidization of binary mixture, one component fluidizes at a lower gas velocity (u_f), while the other component at a higher velocity (u_p). The article explains that during the fluidization process, the lighter or finer component tends to rise, called "flotsam", while the heavier or coarser component tends to sink, called "jetsam". The article also mentions that to estimate the U_{mf} of a binary system, it is necessary to consider the different characteristics of mixing and segregation of two kinds of particles having different properties. Finally, Chiba et al. (1979) classified the mixing state in fluidized bed of binary systems into three cases, which were (a) complete mixing, (b) complete segregation, and (c) partial mixing[22].

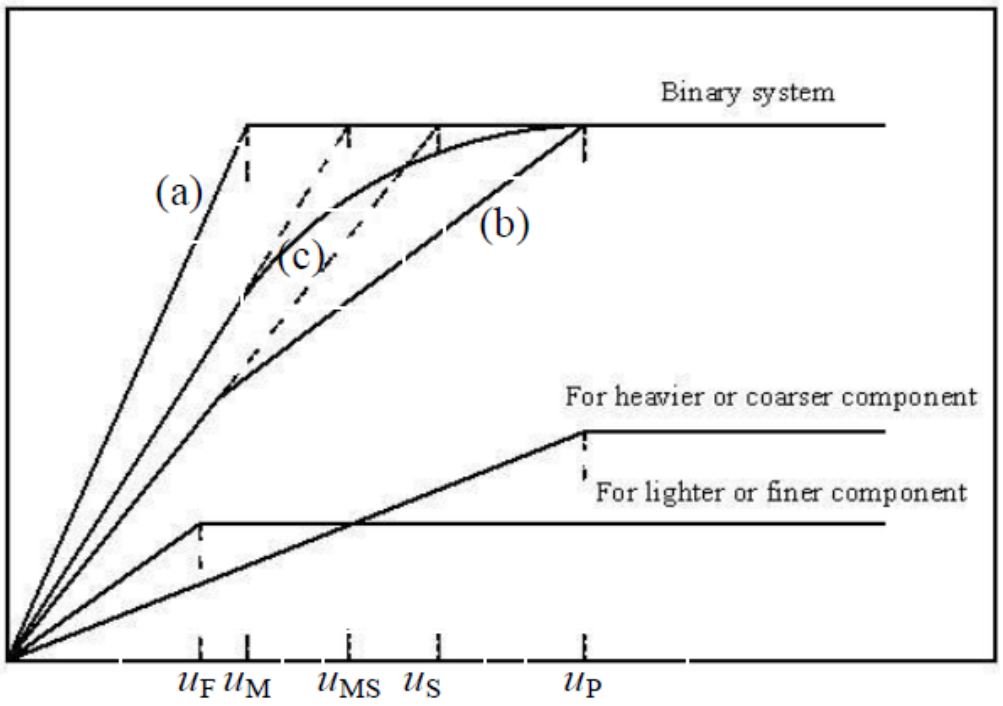

Figure 2.5 Bed pressure drop curve with respect to mixing or segregation state (in an idealized case) a. total mixing, b. total segregation, and c. partial mixing are examples of mixing[23].

In binary particle systems, the influence of various mixing states on the bed pressure curve is shown in Figure 1. Case (a) is in a condition of complete mixing, where all the particles are fluidized to the same extent as a pure component or mixing component made up of particles with essentially the same size and density. The bed in Case (b) is completely segregated, with flotsam at the top and jetsam at the bottom. Case (c) is in a state of partial mixing, which is a transitional condition between Case (a) and Case (b). Case comprises most of the mixing states in real fluidized beds of binary systems (c). The minimum fluidization velocity for a partial mixing fluidized bed is found at the intersection of the two extrapolated linear portions of the plot that correspond to the regions where the entire bed is first fluidized ($u_g > u_p$) and then packed ($u_g < u_f$). As seen in Fig. 1, this u_{mf} of three examples is represented as u_M, U_S, and u_{MS}, respectively[23].

The theoretical calculation of the bed pressure drop under various surface gas velocities in a packed bed is done using Ergun's equation[24]. The Ergun's equation was modified by Wen et al. (1966)[25] to calculate the u_{mf} in a single-component fluidized bed.

$$Ar = 24.5Re_{p,mf}^2 + 1650Re_{p,mf} \tag{2.14}$$

Goosen et al. (1971)[26] defined the average diameter and density of binary particles to employ Eq. (2.15) for binary systems.

$$\frac{1}{\bar{\rho}} = \frac{w_F}{\rho_F} + \frac{1 - w_F}{\rho_J} \tag{2.15}$$

$$\frac{1}{\overline{\overline{d\rho}}} = \frac{w_F}{d_F\rho_F} + \frac{1 - w_F}{d_J\rho_J} \tag{2.16}$$

Further changed by Noda et al. (1986)[27] On the basis of Eq. (1) and the diameter and density of binary particles,

$$Ar = ARe_{mf}^2 + BRe_{mf} \tag{2.17}$$

Where,

$$A = 36.2\left(\frac{d_J}{d_F}.\frac{\rho_F}{\rho_F}\right)^{-0.196}, \qquad B = 1397\left(\frac{d_J}{d_F}.\frac{\rho_F}{\rho_F}\right)^{0.296} \tag{2.18}$$

Using a straightforward equation, Cheung et al. (1974)[28] proposed that for binary particles of equal density,

$$u_{mf} = u_F\left(\frac{u_J}{u_F}\right)x_J^2 \qquad when\ \frac{\rho_F}{\rho_F} < 3 \tag{2.19}$$

The equation Chiba et al. (1979)[22] presented for binary mixture particles with significant size difference,

$$u_{mf} = \frac{u_F u_J}{u_F x_F + u_J(1 - x_F)} \tag{2.20}$$

2.6 Mode of air supply

2.6.1 With Distributor Plate

The air distribution plate is a crucial component in the design of fluidized beds as it supports the bed parts and ensures that the gas flows evenly across the bed. The bed materials, which are typically particles placed on top of the grates, are fluidized by the gas that passes through the grate. The grate has holes and slots that allow the gas to flow through and distribute itself uniformly throughout the bed. The size and arrangement of these holes are vital in maintaining the proper fluidization characteristics of the bed, such as preventing settling or clumping of the particles. As there are no other ways to modify the air distribution through the solids phase after the air distribution grate, the significance of the air distribution plate cannot be overstated. For optimal performance of the fluidized bed, it is important to design and operate the air distribution plate correctly[5].

The flow parameters of a fluidized bed, and therefore mixing and heat and mass transfer accomplished inside it, are directly influenced by distributor design[29]; these features have an impact on the efficacy of many applications.

The picture in Figure 2.6 shows how particles move in a fluidized bed, which is important for mixing. .Stein et al.[30], Laverman et al. [31] and Li et al.[32], who used porous sintered distributors , and they found that certain circulation patterns, like B and D, are better for mixing. However, when the bed is poorly designed, it can lead to less effective mixing, as shown in patterns A and C. In one study, they used a certain type of distributor and found that systems with multiple rolls (like D) mixed the particles better than systems with a single roll (like A).

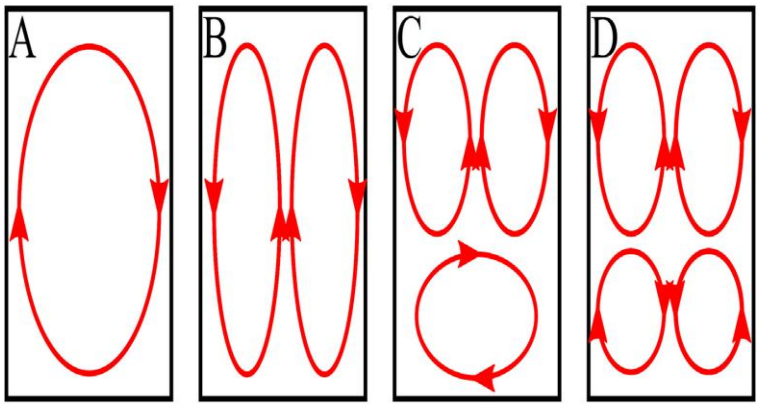

Figure 2.6 The four flow patterns that Li et al.[32] described.

.

2.6.2 Without distributor plate with side two nozzles

In fluidized bed reactors, a distributor plate is often employed to distribute the fluidizing gas evenly throughout the bed. The distributor plate, however, has several drawbacks like as follows,

- Operating expenses rise because of the additional power needed to pump gas through the reactor using a distributor plate.
- The distributor plate's pores may become clogged with fine particles, causing local de-fluidization and dead zones in the reactor. Reactor performance and efficiency may suffer as a result.
- To avoid blockages and ensure functionality, the distributor plate needs to be cleaned and maintained frequently. This may increase downtime and operational costs.
- The choice and creation of an appropriate distributor plate might be challenging, necessitate more resources and labor, and so raise the overall cost of developing and running a fluidized bed reactor.
- When a distributor plate is used, the pressure drop across the reactor may increase, which could raise the cost of gas pumping and decrease efficiency.

As an alternative, the fluidizing gas can be introduced into the reactor by orifices or nozzles, which can be located at the bottom of the reactor or on the reactor's side wall[1].

There is limited research on the performance of a fluidized bed reactor without a gas distributor. Large particles at the bed's bottom serve as a gas distributor in experiments done by Agu et al. (2018)[33] to operate a fluidized bed reactor without a gas distributor. Their study's objective was to investigate the solid’s dispersion in a fluidized bed that wasn't using a gas distributor. According to the findings of their research, the bed that wasn't operated by a gas distributor had a more uniform distribution of solids than the bed that was.
As an alternative, gas can be fed to the reactor by orifices or nozzles, which can be located at the bottom of the reactor or on its side. To ensure the reactor runs without a hinder, this approach also needs to characterize the fluidized bed behavior for gas flow boundary conditions. The benefit of this approach is that it can reduce the cost of the gas distributor's construction and design as well as its running expenses. To guarantee the reactor runs without

a hitch, it is crucial to characterize the fluidized bed behavior for the stated gas flow boundary conditions (Sasic and Johnsson, 2005)[34].

3 Materials and Methods

For experimental investigation to be carried out successfully, choosing the right materials is essential. Geldart B and Geldart D particles were selected for use in the bubbling fluidized bed reactor experiment. The range of sizes, densities, and composition of these particles were taken into consideration because these factors have a significant impact on the hydrodynamic behavior of fluidized beds.

3.1 Geldart B

Silica sand particles shown in figure 3.1 represent the Geldart B particle, a dense particle. Utilizing sieve analysis, the mean diameter and particle size distribution of silica sand particles were determined.

Figure 3.1 Silica Sand particle of diameter 850-1000 microns

Summary of the silica sand particle's characteristics is listed in Table 3.1

Table 3.1 Properties of Silica sand particle.

Mean Diameter	850-1000 microns
Density	2650 kg/m^3
Bulk Density	1222 kg/m^3
Solid Void Fractions	0.54

3.2 Geldart D

Timber pellets were chosen as shown in figure 3.2, for the Geldart D particle. The results of the examination of the timber pellets' composition at Eurofins' testing laboratory are displayed in Table 2 and Table 3 provides summary of the timber pellets characteristics.

Figure 3.2 Timber Pellets

Table 3.2 Composition of Timber Pellets.

Ultimate analysis (%)	Timber Waste Pellets	
	Moisture Free	Delivered
Carbon	50.7	42.3
Hydrogen	5.7	6.6
Oxygen	39	47.2
Nitrogen	1.08	0.9
Sulphur	0.045	0.037
Ash	3.34	2.78
Volatile	78.4	65.4
Moisture	NA	16.6

Table 3.3 Properties of Timber Pellets.

Mean Diameter	Approx. 8 mm
Density	1086 kg/m^3
Bulk Density	500 kg/m^3

These particles were chosen to study the fluidization behavior of binary mixtures because of their distinct properties, i.e., size, shape, density, and composition.

4 Experimental Setup and Procedure

4.1 Construction of fluidized bed reactor with side nozzles as inlet boundary conditions

To achieve the objective of thesis, firstly the bubbling fluidized bed reactor with side nozzles as inlet flow boundary condition was constructed through process of steps which is descried below.

4.1.1 Design

The bubbling fluidized bed reactor was constructed using a cylindrical tube with a diameter of 10 cm that was available in the lab. Before the construction of reactor, a 3D model was made by AutoCAD drafting software as shown in Figure 4.1.

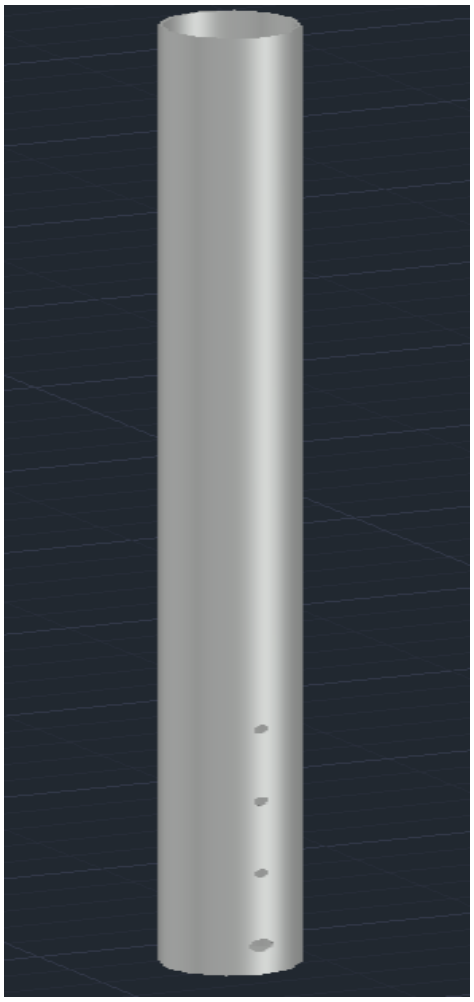

Figure 4.1 AutoCAD draft.

4.1.2 Construction

After proper design of reactor then firstly tried to make holes for nozzles using a drilling machine with a normal standard bid. However, because a standard drill bed was used, a lot of glass was damaged during the drilling process. To solve this issue, a tapering drill bed was employed, which made it possible to drill the holes in the glass without breaking it. After making the holes in reactor, threads in the holes were created by using a thread die and tap set instrument for fit nozzles in those holes. Here upper end of reactor left open whereas lower end of reactor is closed by using circular slab.

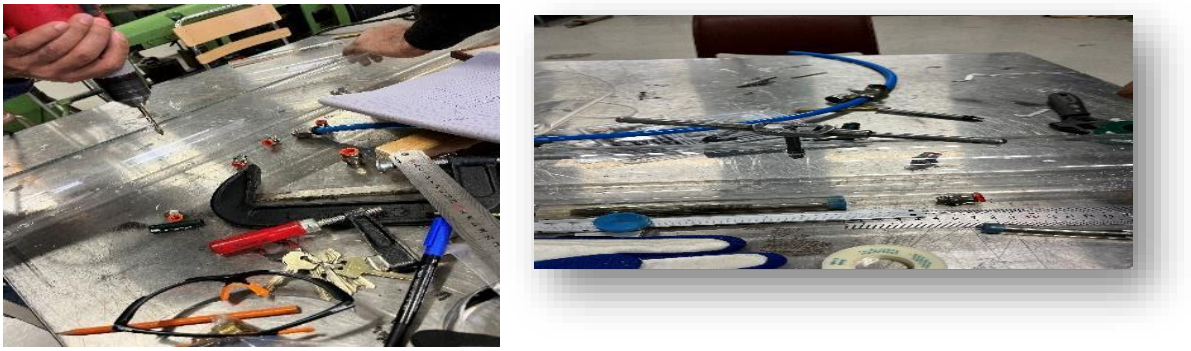

Figure 4.2 Construction of fluidized bed

Figure 4.3 Installation of nozzle

4.1.3 Challenges

The use of a standard drill bit during construction caused a lot of glass to break, making it very challenging to drill the holes. However, this issue was resolved by use a tapering drill bit. Similarly, there was a problem in making the thread in the holes, but it was resolved by using a thread die and tape set.

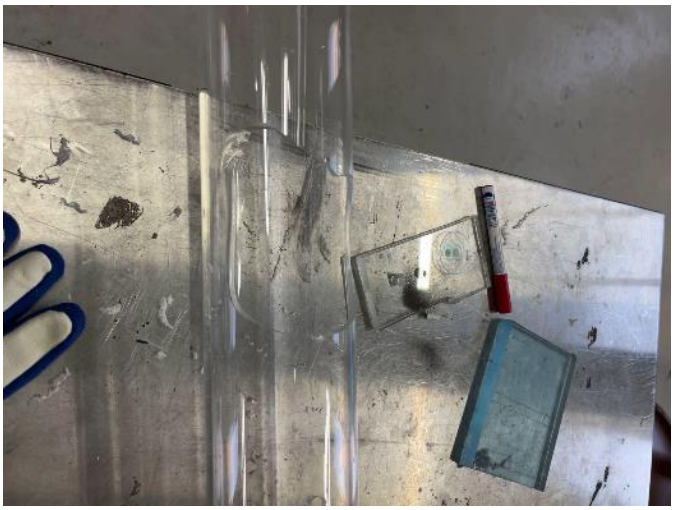

Figure 4.4 *Breakage of the tube during drilling by normal bit.*

Dimensions of the Bubbling Fluidized Bed Reactor with Side Nozzles are listed in Table 4.1.

Table 4.1 Dimensions of the Bubbling Fluidized Bed Reactor with Side Nozzles.

Parameter	**Dimension**
Diameter of Reactor	10 cm
Length of Reactor	130 cm
Diameter of nozzle	12 cm
Nozzle distance from bottom end	4 cm
Distance between the pressure measurement points	10 cm

4.2 Equipment

Two bubbling fluidized bed reactors, one with the distributor plate and the other with two side nozzles, made up the experimental setup. The reactors were set up in the university's process hall in Porsgrunn, South-Eastern Norway. The experiments were conducted to determine how well the two reactors performed under identical operating circumstances.

4.2.1 Bubbling fluidized bed reactor with the distributor plate

The experimental setup in a bubbling fluidized bed reactor with a distributor plate consists of a transparent cold bed reactor with a diameter of 8.4 cm and a height of 140 cm. To ensure even gas flow through the bed, a distributor plate with a diameter of 8.4 cm and a thickness of 3 mm was connected 4 mm from the bottom of the reactor. At 10 cm intervals, pressure transducers were placed along the column's wall to collect data on the pressure distribution inside the column. Through an air supply pipe at the base of the column, compressed air was delivered to the reactor. A control valve attached to the rig controls the air flow rate.

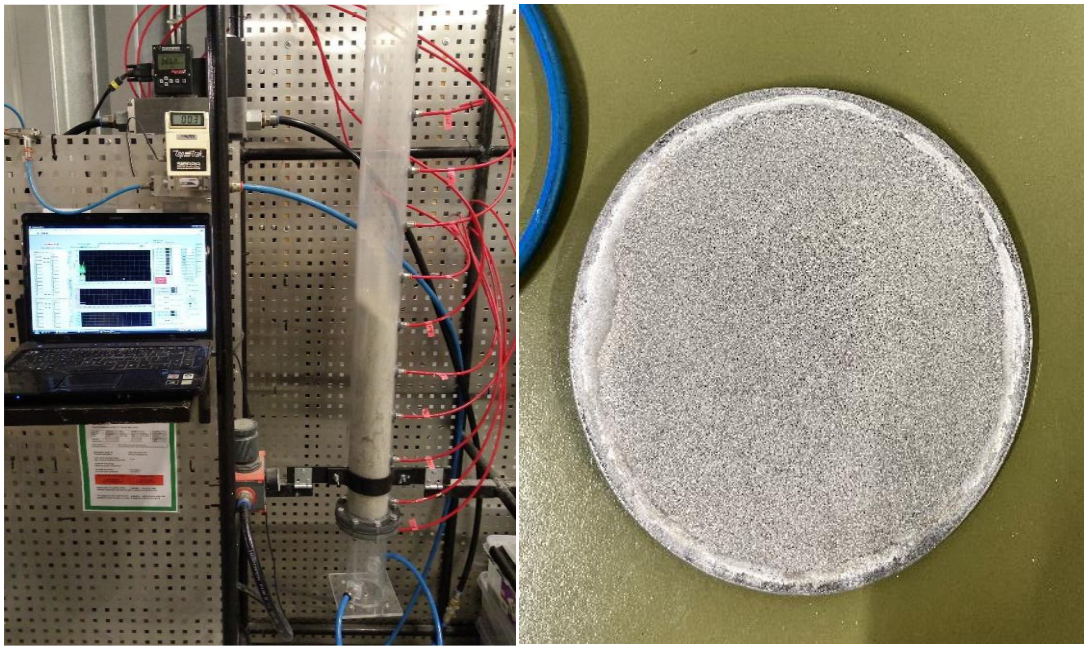

Figure 4.5: (a) Left fluidized bed reactor with distributor plate, (b) Right distributor plate.

4.2.2 Fluidized bed with two side nozzles as inlet boundary conditions

For the experimental setup in the reactor with side nozzles, the newly constructed reactor was used. Like in the reactor with the distributor plate, pressure transducers were installed along the wall of the column. They were installed at 10 cm between two consecutive pressure points along the column height in the reactor. Compressed air was supplied to the newly constructed reactor through air supply hoses fitted on both sides of the column nozzle, and the airflow rate was controlled by a control valve attached to the rig.

Figure 4.5 Fluidized bed reactor with two side nozzles as inlet boundary conditions.

4.3 Procedure

Particles were added to the column from the top before the experiment began. The control valve was then progressively turned up to gradually raise the surficial velocity, which was compressed air at ambient conditions. Using pressure sensors mounted to the cold bed column, the pressure drop caused by the velocity increase was recorded in LabVIEW. And then, data from LabVIEW is analyzed from the MS Excel.

A minimum of 60 seconds was given for the flow to establish itself before collecting data, and data were gathered for each flow rate for more than a minute with a sample time of one second. The particles were taken out of the column after each experimental series because once fluidized, fluidized bed particles have different properties.

The pressure drop at each tapping point for each flow rate was calculated by subtracting the distributor pressure at the corresponding flow rate. This is shown in equation 4.1.

$$\Delta P_{1,f_i} = P_{1,f_i} - P_{2,f_i} \tag{4.1}$$

Where P_1 pressure at a pressure tapping point 1,
P_2 pressure at a pressure tapping point 2,
f_i air flow rate.

4.4 Experiments

4.4.1 Experiment on fluidized bed reactor with a distributor plate

In bubbling fluidized bed reactor with distributor plate, a series of experiments were conducted using different percentages of bed particles as shown in table 4.2 by sand only and biomass to sand particles in ratios of 5%, 10%, and 15%.

Table 4.2 Experimental conditions for bubbling fluidized bed reactor with distributor plate.

Mixture	Weight percent of biomass	Weight of sand	Weight of biomass	Initial bed height
Sand only	0	1795g	0	17 cm
Sand and biomass	5%	1795g	89.75 g	18.6 cm
Sand and biomass	10%	1795g	179.5 g	20 cm
Sand and biomass	15%	1795g	269.25 g	21.8 cm

4.4.2 Experiment on fluidized bed reactor with side nozzles as inlet boundary conditions

A series of experiments were conducted in the reactor with two sides nozzles, first only with sand as bed particles and then by increasing the ratio of biomass and sand particles 5%, 10% and 15% respectively as shown in Table 4.3.

Table 4.3 Experimental conditions for the bubbling fluidized bed reactor with side nozzles.

Mixture	Weight percent of biomass	Weight of sand	Weight of biomass	Initial bed height
Sand only	0	1955g	0	20 cm
Sand and biomass	5%	1955g	97.75 g	21.3 cm
Sand and biomass	10%	1955g	195.5 g	22.7 cm
Sand and biomass	15%	1955g	293.25 g	24.2 cm

5 Simulation setup

Studying the movement of particles through fluids in experiments is often limited by factors such as complex geometry, extreme operating conditions, and difficulties in observing the inner workings of the process. Using experimental methods can be costly and inefficient when compared to simulations, which are capable of addressing these challenges in a faster and more convenient manner.[7]. In this study, we created the hydrodynamic flow regimes in a 10 cm bubbling fluidized bed reactor using the Computational Particle Fluid Dynamic (CPFD) program Barracuda VR@21.0.1.

5.1 Simulation setup

5.1.1 Geometry and Grid Setup

A cylindrical CAD geometry was imported in Barracuda VR software which have a diameter of 10 cm and a height of 400 cm. A uniform grid of total cell 18,000 was established around the geometry around for the simulation. To maintain numerical stability throughout computation, cells with volume fractions less than 0.04 and aspect ratios more than 15:1 were eliminated. To track pressure, particle volume fractions, mass concentrations, fluid velocity, and other variables, monitoring points were chosen at the center of the column and at a height that corresponded to the pressure transducer's position in the experiment. Figure 5.1 depicts the grid and CAD layout, transient data locations, and simulation settings for the reactor.

Figure 5.1 (a) Grid and Cad figure (b) Transient data location in column.

5.1.2 Global setting

The simulations were carried out with an ambient temperature of 300K as the constant temperature. Gravitational acceleration in the Z-direction was kept constant at -9.8 m/s.

5.1.3 Base Material definition

For the first simulation, silica sand (SiO_2) was considered as the base material. Further simulations were run with a mixture of sand and biomass in different weight percentages.

5.1.4 Particle size and Drag Model

The sand particles used for simulation had a density of 2650 kg/m3, a sphericity of 0.85, and a diameter of 750–1000 microns. The biomass particles had a density of 1086 kg/m3, a sphericity of 0.5, and a diameter of 6 to 8 mm. The EMMS-Yang-2004 drag model was applied to the reactor with side nozzles.

5.1.5 Initial conditions

Table 5.1 Operating Conditions

Fluidizing Gas	Compressed air
Fluid Temperature	300K
Superficial Gas Velocity	0-0.7 m/s
Outlet Pressure	101325 Pa

5.1.6 Flow and Pressure boundary conditions

The top end of the column was configured as pressure boundary conditions for the reactor with side nozzles. The side nozzles 4 cm from the bottom end of the column were configured as inlet flow boundary conditions. The bottom of the column was used as the inflow flow boundary condition for the reactor with a uniform distribution. The top of the column was considered as the pressure boundary condition, as in the experimental setup shown in Figure 5.2.

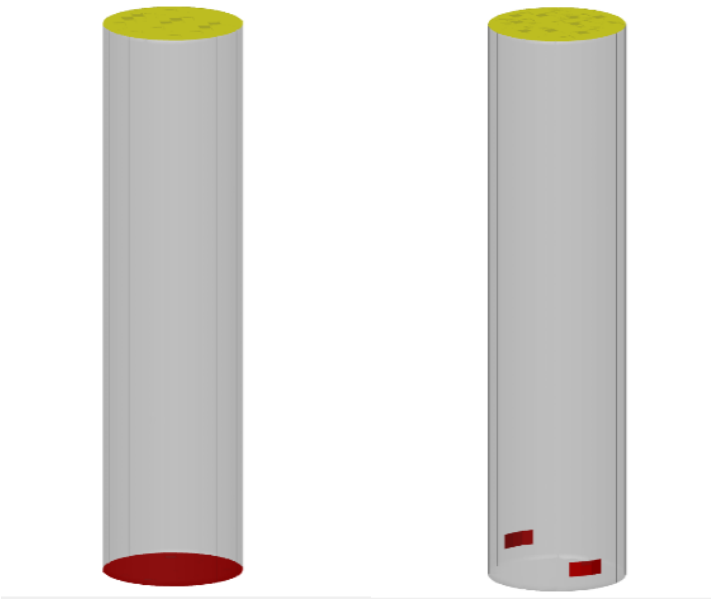

Figure 5.2 (a) Left side is the flow and pressure boundary condition for the reactor with side two nozzles and (b) Right is the flow and pressure boundary condition for the reactor with uniform distribution.

5.1.7 Simulation in hot bed conditions

For hot bed conditions, bed temperature was maintained at 700 C, biomass was fed at a rate of 0.00083 kg/s and the air was supplied at 0.00128 kg/s.

5.1.8 Simulation Time, Data Output and Post-Processing

0.01 seconds was chosen as the visualization data output plot interval to produce high-frequency and real-time animations. To fully capture flow hydrodynamics and attain steady-state conditions, a simulation time of 400 seconds at a 0.001 sec time step was selected for all simulations for the cold bed, and for the hot bed simulation time was taken 120 with a time step of 0.001 sec. The data post-processing software was Tecplot 360 and Microsoft Excel.

6 Results and Discussions

The purpose of this chapter is to present and discuss the results obtained from the experiments and simulations conducted on a bubbling fluidized bed reactor with two side nozzles and with uniform distribution as distributor plate in experiments. And compare the results of both reactors from results through experiments and simulation too, together with a thorough analysis of the implications and importance of the findings.

6.1 Experimental results

6.1.1 Minimum Fluidization velocity

6.1.1.1 Minimum fluidization velocity comparison between binary mixture

The minimum fluidization velocity for biomass particles made of sand and biomass was examined in this study for four different mixtures with sand. The mixtures had weight percentage ratios of biomass and sand particles 0%, 5%, 10%, and 15%. The experimental data were obtained by plotting pressure drop versus superficial gas velocity for sand, sand, and 5% biomass, sand and 10% biomass, and sand and 15% biomass. Figures 6.1 and 6.2 show the change in pressure drop with respect to the change in superficial gas velocity for all four mixtures for fluidized bed reactor with two side nozzles as inlet boundary conditions and fluidized bed reactor with uniform distribution respectively.

Figure 6.1 shows that the minimum fluidization velocity values were 0.25 m/s, 0.24m/s, 0.23m/s, and 0.21m/s for sand, 5% biomass and sand, 10% biomass, and sand and 15% biomass respectively for fluidized bed reactor with side nozzles.

Whereas from Figure 6.2 show the minimum fluidization velocity values were 0.36 m/s, 0.34 m/s, 0.33 m/s, and 0.31 m/s for sand only, sand and 5% biomass, sand and 10% biomass, and sand and 15% biomass, respectively, for the fluidized bed reactor with a distributor plate which is higher than minimum fluidization velocities of the reactor with side nozzles.

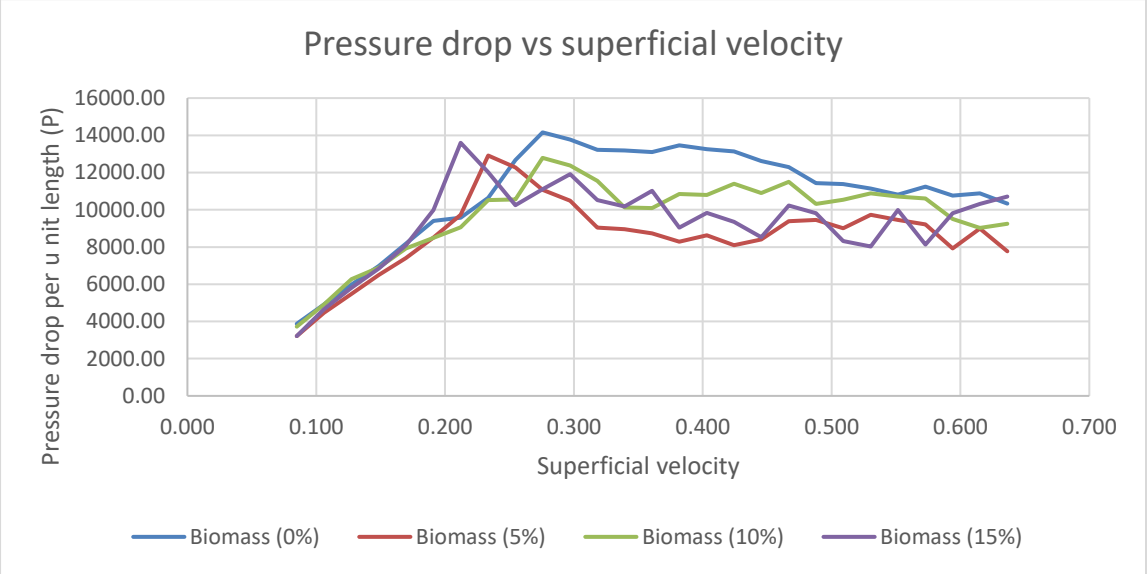

Figure 6.1 Minimum fluidization for sand and biomass particles on increasing percentage in fluidized bed reactor with side nozzles.

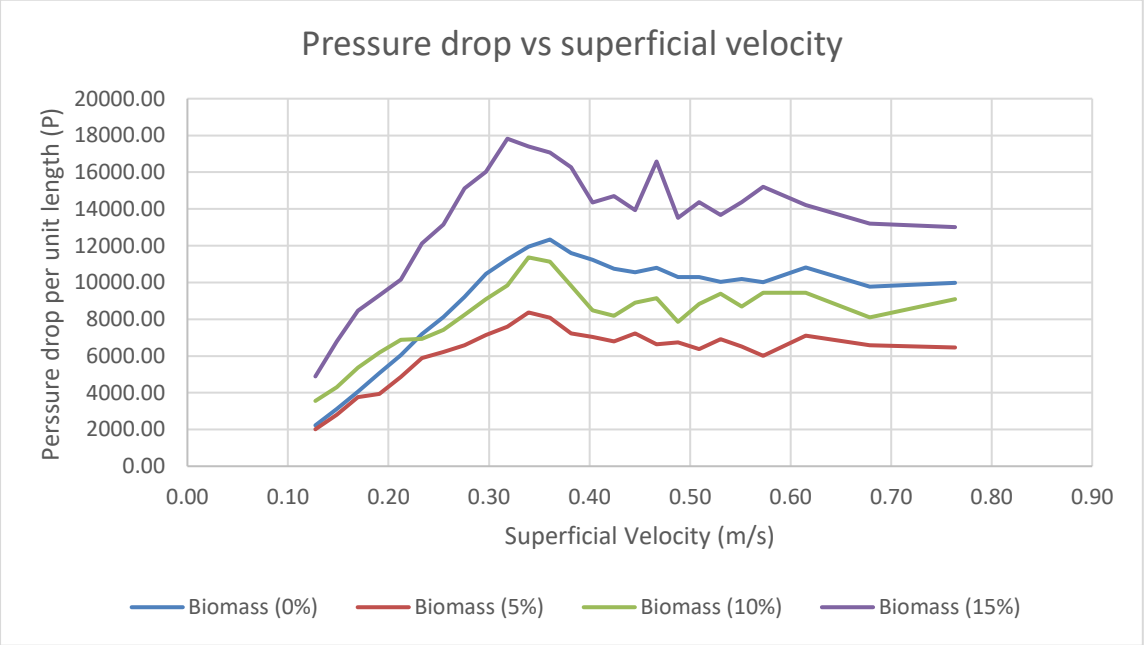

Figure 6.2 Minimum fluidization for sand and biomass particles on increasing percentage in fluidized bed reactor with uniform distribution.

The results indicate that when biomass particles are added to sand particles, the minimum fluidization velocity of binary mixtures goes on decreasing because biomass is less dense and has more surface area compared to sand. The higher surface area of the biomass particles leads to more gas-solid contact and greater fluidization, while the lower density of the biomass particles results in a lower pressure drop at the same superficial gas velocity.

Further, with increasing biomass mass in the mixture, there is an increasing fluctuation in pressure drop per unit length vs superficial gas velocity. The reason for this is that binary mixtures behave differently from sand alone. In the case of sand and biomass, sand particles are denser than biomass particles. Therefore, at low superficial velocities, the sand particles settle down and form a dense bed at the bottom of the fluidized bed. As the superficial velocity increases, the pressure drops across the bed increase, and the bed expands. However, biomass particles tend to get carried away with gas flow due to their lower settling velocity. This leads to a non-uniform distribution of biomass particles in the fluidized bed, resulting in fluctuations in the pressure drop per unit vs superficial velocity.

In contrast, in the case of sand particles alone, the settling velocities of all sand particles are similar. This leads to a more uniform particle distribution in the fluidized bed. As a result, for sand particles, the pressure drop per unit vs superficial velocity curve is relatively steady.

.

6.1.1.2 Minimum fluidization velocity comparison between the reactors

To study the hydrodynamic behavior of new the fluidizing bed reactor with side nozzles, the minimum fluidization velocity for sand particles was studied in two different types of fluidized bed reactors, one with two side nozzles and the other with a distributor plate.

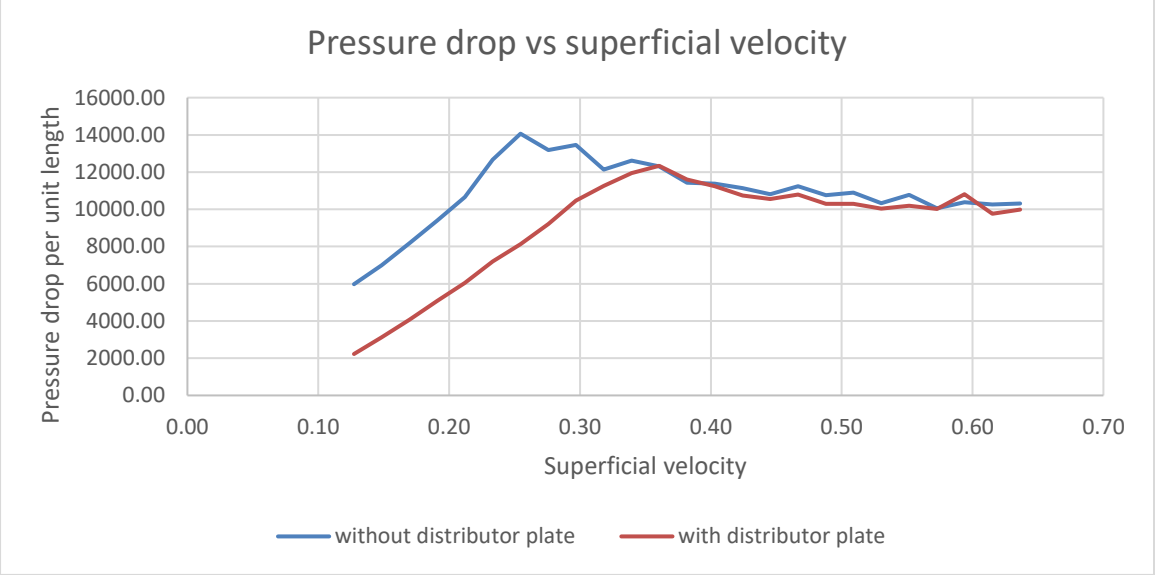

Figure 6.3 Minimum fluidization velocity comparison between fluidized bed reactor with side nozzles vs with distributor plate

According to the results, the fluidized bed reactor with a distributor plate had a higher minimum fluidization velocity (0.36 m/s) than the reactor with two side nozzles (0.25 m/s). This can be attributed to the distributor plate's ability to distribute gas flow more evenly across the bed. This creates a high-pressure drop across the bed, which increases the minimum fluidization velocity.

In contrast, in the case of the reactor with side nozzles, gas may channel through a bed creating a preferential path. Fluidizing gas doesn't passed through a whole bed resulting in less pressure drop across the bed and lowering the minimum fluidization velocity.

6.1.1.3 Mixing and Segregation comparison

During the experiments, I observed the approx. value of good mixing velocity range and after what approx. velocity binary mixture starts to segregate. So, Table 6.1 depicts mixing and segregation properties among the binary mixture of 5%, 10% and 15% of biomass with sand particles and between the bubbling fluidized bed reactor with two side nozzles and bubbling fluidized bed reactor with distributor plate.

Table 6.1 mixing and segregation properties comparison among binary mixtures and reactors.

	BFBR with distributor Plate	BFBR without distributor Plate
Good mixing properties (5% biomass)	Velocity from 0.35m/s to 0.39 m/s	Velocity from 0.25m/s to 0.32 m/s
Good mixing properties (10% biomass)	Velocity from 0.33m/s to 0.38 m/s	Velocity from 0.23 m/s to 0.29 m/s
Good mixing properties (15% biomass)	Velocity from 0.31m/s to 0.35 m/s	Velocity from 0.22m/s to 0.26 m/s
Segregation (5% biomass)	segregates from approx. from 0.4 m/velocity	segregates from approx. from 0.33 m/velocity
Segregation (10% biomass)	segregates from approx. from 0.38 m/velocity	segregates from approx. from 0.31 m/velocity
Segregation (15% biomass)	segregates from approx. from 0.35 m/velocity	segregates from approx. from 0.27 m/velocity

Regarding the mixing and segregation properties among the binary mixture in both reactors, the mixing between biomass and sand particles is quite good closer to the minimum fluidization velocity and has a wider range of superficial velocity for good mixing found on 5% and gradually decreases range on increasing the biomass percentage whereas segregation starts to appear faster in binary mixtures of larger biomass percentages.

The good mixing properties and closer proximity to minimum fluidization suggest that the fluidized bed may not over-fluidized. And at the same time, sand and biomass particles are suspended by strong fluidization, facilitating effective mixing. And lower biomass percentages (say 5%) are expected to provide a wider range of favorable mixing qualities since the biomass particles are spread out more uniformly in the fluidized bed at these lower concentrations.

Because of this, sand and biomass particles interact with greater frequency, which improves mixing. Additionally, the larger and less dense biomass particles tend to move upward more quickly in the fluidized bed as the biomass content rises compared to the smaller and denser sand particles. The larger biomass particles tend to collect near the top of the bed, which causes further segregation between the two types of particles. In the case of segregation, the larger and less dense biomass particles, compared to the smaller and denser sand particles, tend to rise more quickly in the fluidized bed as the biomass percentage increases. As a result of the larger biomass particles likely to collect near the top of the bed, there is more segregation between the two types of particles.

According to the results of comparing the mixing and segregation characteristics of the two reactors, the reactor with two side nozzles may provide better mixing performance for the different percentages of binary mixtures because it requires less minimum fluidization velocity than the reactor with a distributor plate as it requires less energy to initiate fluidization and suspension of the particles. This lower velocity might improve mixing and reduce particle entrainment. In contrast, the reactor with a distributor plate has a higher minimum fluidization velocity, which may need more energy to start fluidization and increase particle entrainment and segregation. But in the case of the reactor with two sides nozzles mixing occurs mainly on the upper part of the bed as there is a dead bed section in the lower region of the reactor. Whereas, due to the absence of a dead bed zone in the reactor with the distributor plate, mixing was seen in the whole bed.

6.1.1.4 Some difference seen in between the reactors.

Several differences between the two reactors were seen during the experiments. The most noticeable of these were:

6.1.1.4.1 Bubbles rising patterns.

In two different kinds of bubbling fluidized bed reactors, various patterns of rising bubbles were seen during the fluidization process. Small bubbles were initially rise only from the sides of the first type of reactor, which had side nozzles, but in later some bubbles were noticed rising from the center of reactor as well. However, bubbles were seen rising all over the reactor during and after fluidization in the type of reactor with a distributor plate.

Here, in case of bubbling fluidized bed reactor with side two nozzles, during the lower superficial velocity of air, it just passes through the sides of nozzles as it air is supply through sides only and it has overcome the more drag forces in center which will not be enough but when the superficial velocity is high enough, it passes all over from the reactor as it has sufficient forces for expansion of bed. But incase reactor with distributor plate, gas is introduced evenly across the whole bed of a bubbling fluidized bed reactor with a distributor plate using the perforations in the plate. As a result, bubbles start to form all over the bed, including the center and the sides at just minimum fluidization velocity and at higher superficial velocity.

6.1.1.4.2 Motion of bed materials

Motions of bed particles in reactor in both reactors is shown in Figure 6.4. In the fluidized bed reactor with side nozzles, only upper part was in movement, but lower

parts show no movement in a dead bed zone section. On the other hand, the entire bed was in motion in the bubbling fluidized bed reactor with a distributor plate.

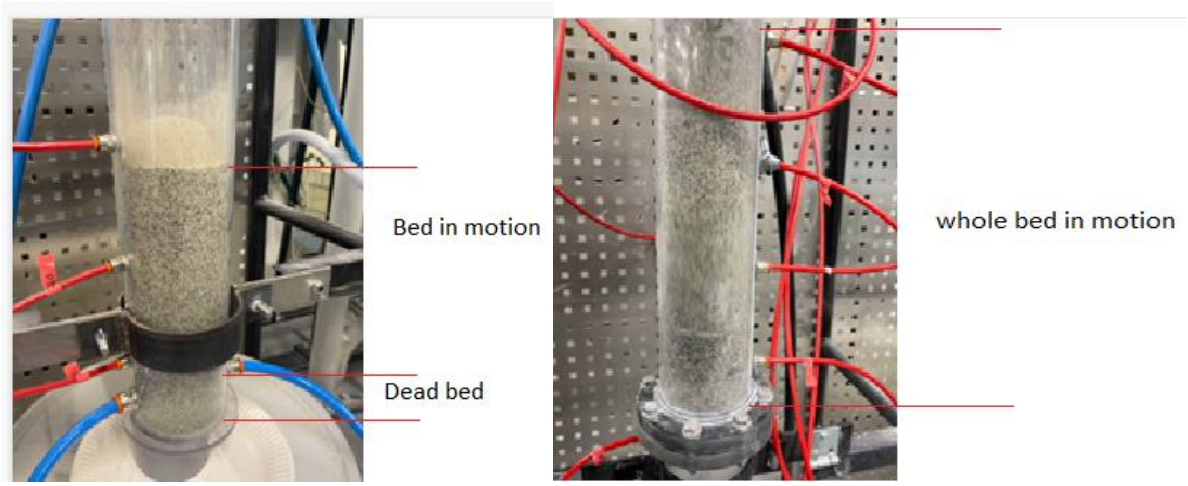

Figure 6.4(a) Left side of figure fluidized bed reactor with two sides nozzles partially in motion (b) Right side of figure fluidized bed reactor with distributor plate fully in motion.

For the case of reactor with side nozzles, the lower part of the end is at rest during slugging and turbulent regime as shown in Figure 6.4 a, it is because the fluidizing gas was supplied from a bit higher part of the reactor as the nozzle was installed 4 cm form from the bottom end of the reactor. And above the dead zone, all bed particles were in motion. But in the case of the reactor with the distributor plate, there is no dead zone formation because fluidizing gas was supplied from the bottom end of the reactor, so all the bed particles were motion in sluggish and turbulence regimes.

6.1.1.4.3 Preferential Paths

Figure 6.5 show the preferential path in a bubbling fluidized bed reactor. Here, preferential paths were only seen on the bubbling fluidized bed reactor with two side nozzles. On the other hand, this was not the case for the reactor with the distributor plate.

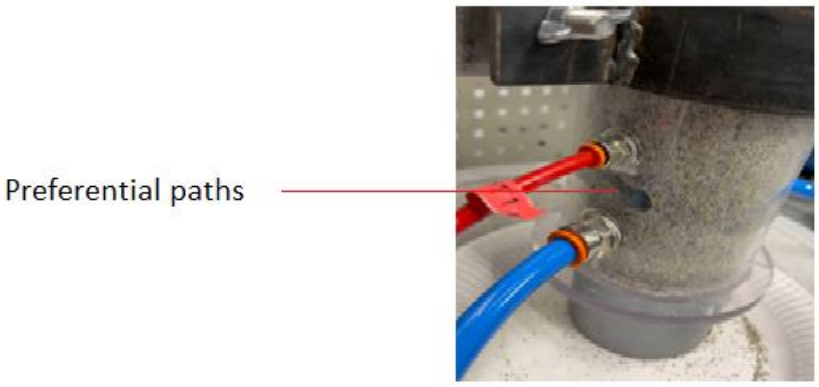

Figure 6.5 Preferential paths in bubbling fluidized bed reactor with side nozzles

In the case of the reactor with side nozzles, the fluidizing gas enters the reactor through two inlets on opposite sides of the reactor. The nozzle hole diameter is larger compared to the reactor with the distributor plate which results in low-pressure flow in the nozzle-type reactor. Therefore, it creates pathways and channels through which gas flows more easily. In contrast, the reactor with the distributor plate air flow through narrowed multiple holes. As a result, no preferential paths were seen.

6.2 Simulation Results

6.2.1 Model Validations

To establish a valid model for further simulation, experiments and simulations were carried out with sand particles. Different drag models were tested to validate a model for simulating the behavior of a newly built bubbling fluidized bed reactor with two side nozzles (10 cm diameter) and the results were compared by plotting pressure drops versus superficial gas velocity as shown in Figure 6.6. The EMMS-Yang-2004 drag model was determined to be the best fit among the various drag models since it predicted values that were closer to the experimental results of the reactor with two side nozzles, with a variation of only 9.5%.

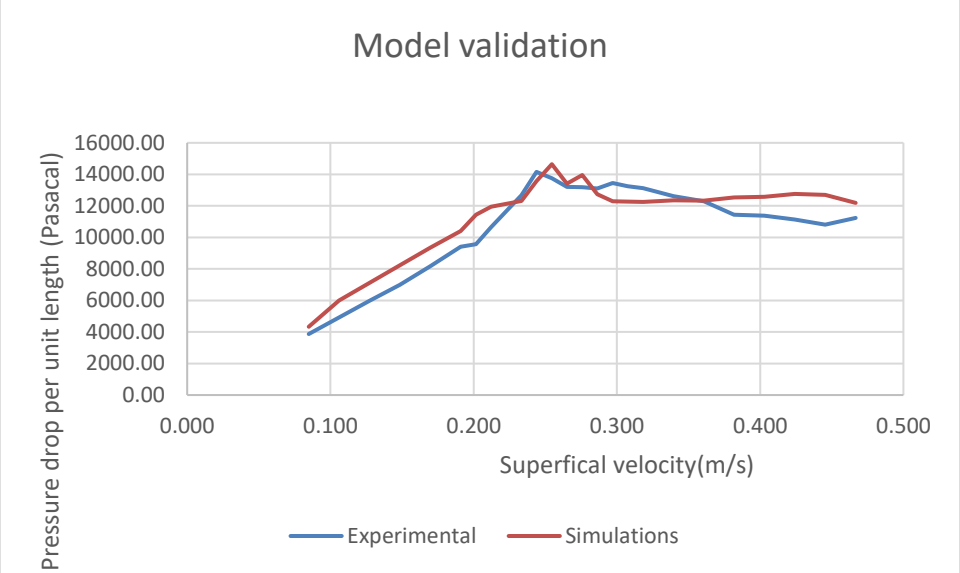

Figure 6.6 Model validation of simulation result with experimental data of reactor with side nozzles

Further simulations were carried out with different percentages of binary mixtures (mixture of 5% biomass and sand, 10% biomass and sand, and 15% biomass and sand) to find the least deviation from the experimental results. When the data were examined, it was found that the 10% biomass and sand mixture had the best fit to the model, with a less deviation by value 708.7 kpa/m of pressure drop per unit length while the other mixtures, which were the 5% and 15% mixtures, had deviations of 1887.76 kpa/m and 1147.31kpa/m, respectively as shown in Figure 6.7. So, on these results basis, 10% biomass and sand particles were for further investigation for a better understanding of both reactors.

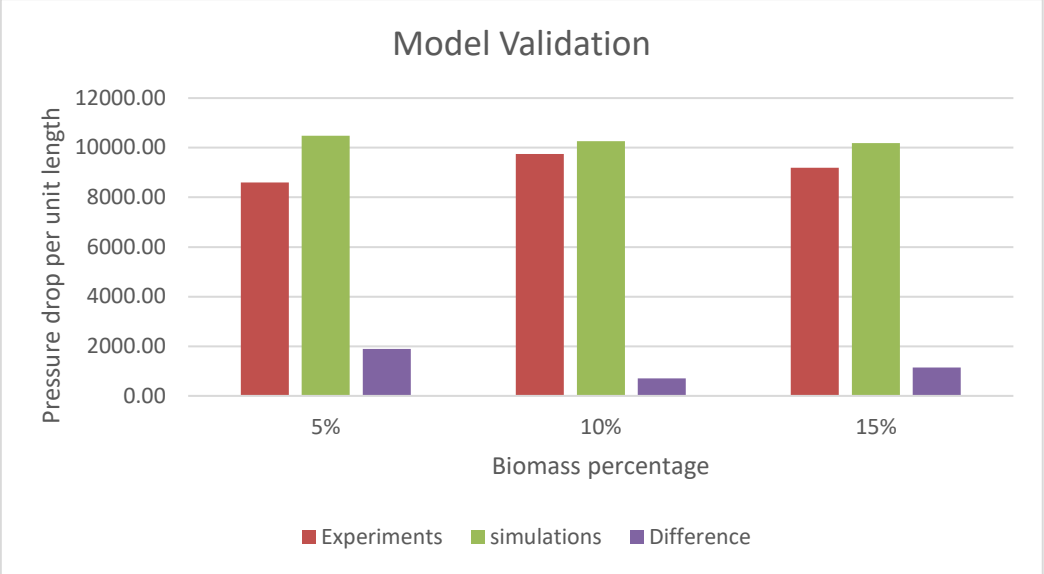

Figure 6.7 Average pressure comparison between experimental and simulation data of different percentage of biomass of reactor with side nozzles

6.2.2 Bubbles behavior

Figure 6.8 (a) displays the cell volume fractions of particles in a bed with two side nozzles on the left-side reactor and a uniform distribution on the right-side reactor. Fig. 6.8 (b) shows the section view of the isosurface of a particle's cell volume fractions. The superficial velocity was kept constant at 0.4 m/s for both reactors in Figure 6.8 (a) and 0.43 m/s in Figure 6.8 (b). From the figure, it shows that large bubbles emerge from the nozzles and move to the surface from the side of the reactor whereas in the case of the reactor with uniform distribution, the center, and sides of the reactor in the reactor with the uniform distribution are filled with smaller bubbles in higher numbers. These findings also observed similar results with the isosurface of the cell volume fractions of particles in the bed.

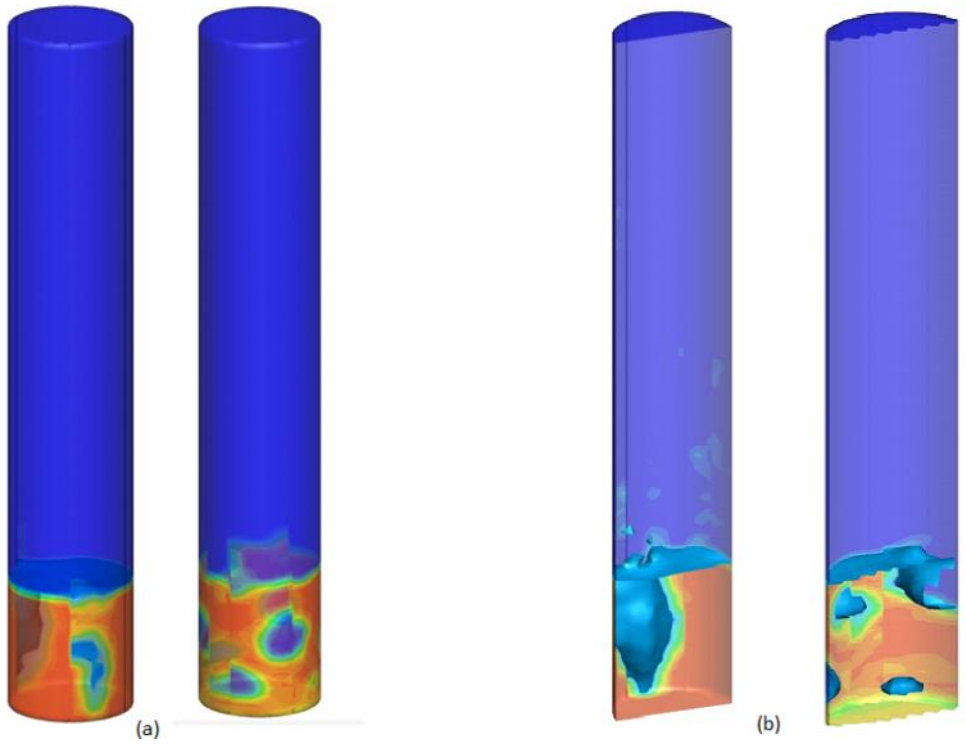

Figure 6.8 (a) Cell volume fractions of bed left sides reactor with side nozzles and right side with uniform distribution

(b) Section view of iso surface of particle volume fraction left side with side nozzle and right side with uniform distribution

In the case of the reactor with two side nozzles, the gas is directly fed into the bed of the reactor by means of side nozzles, causing the gas to enter deeper into the bed and form bigger bubbles and, there are higher velocity and creating the shear forces that cause the gas to be smashed into larger bubbles. Additionally, larger bubbles may gather near the wall, improving gas holdup. But the reactor with a uniform distribution provides a uniform distribution of gas, so smaller and more numerous bubbles appear in the bed.

6.2.3 Mixing and Segregation of particles

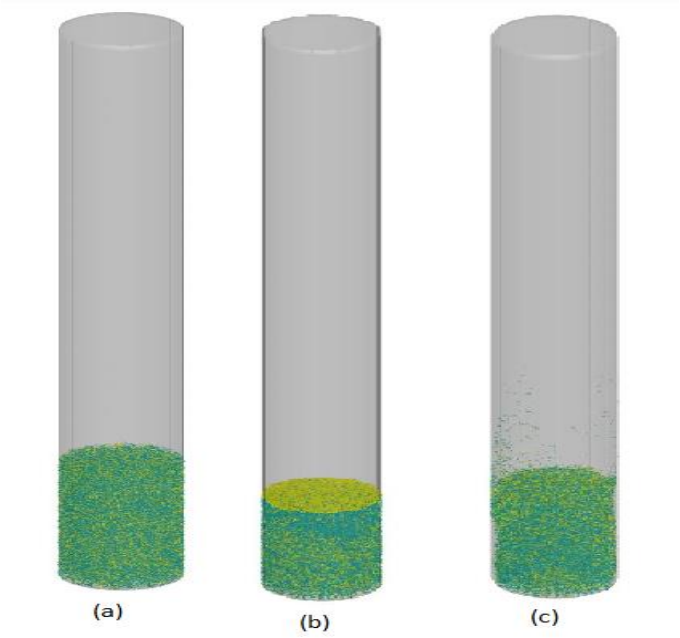

Figure 6.9 Mixing and segregation state of reactor with two side nozzles (a) initial state of particles (b) A final partial segregation of particles (c) Mixing state of particles.

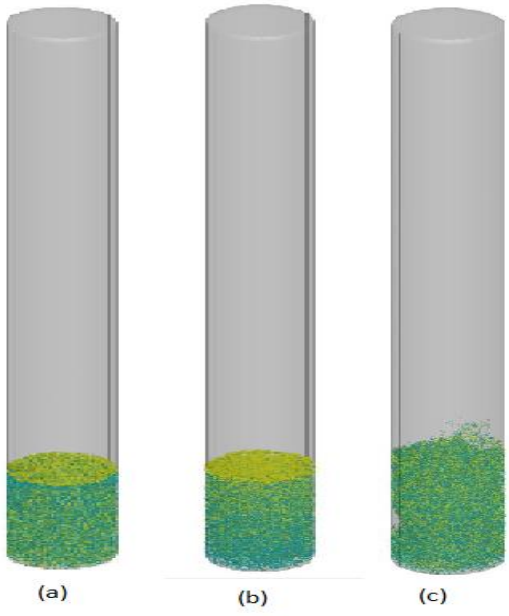

Figure 6.10 Mixing and segregation state of reactor with uniform distribution (a) localized segregation of particles (b) A final partial segregation of particles (c) Mixing state of particles.

Figures 6.7 and 6.8 depict the mixing and segregation behavior of particles in the bubbling fluidized bed reactor with two side nozzles and the distributor plate respectively. In these illustrations, the yellow and green particles correspond to biomass and sand, respectively.

While the reactor with a uniform distribution had clear localized segregation in the initial condition, the reactor with side nozzles displayed a minor level of localized segregation. As the process continued, biomass was segregated from the middle transverse section of the reactor with side nozzles. In contrast, biomass from sand particle segregation was more obvious and started from the bottom of the reactor with a uniform distribution. Furthermore, mixing was seen throughout the reactor in the case of the reactor with a uniform distribution. However, mixing was primarily seen from the sides of the reactor in the reactor with side nozzles.

6.2.4 Particle Volume Fraction

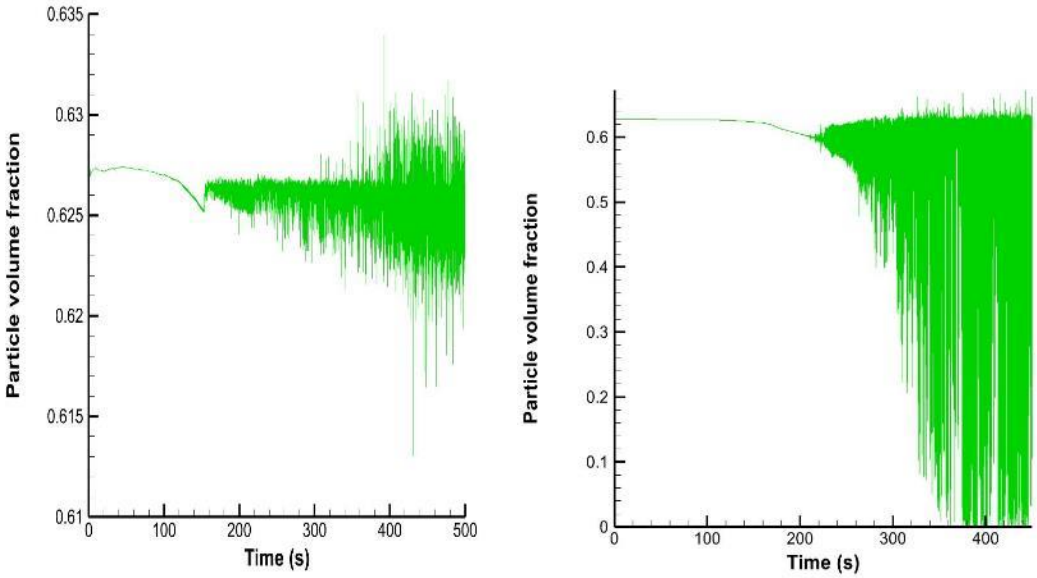

Figure 6.11 Particle Volume fractions fluctuation vs time (a) The reactor with two side nozzles (b) The reactor with uniform distribution.

Figure 6.9 illustrates the particle volume fractions fluctuations with time in reactor with side nozzle in left side and reactor with uniform distribution in right side. From figure it shows that there are large fluctuations in reactor with uniform distribution compared to reactor with side nozzles.

Fluidizing gas is released into the reactor at two locations in a reactor with two side nozzles. Near the nozzles, this causes a confined upward flow of gas and particles, which encourages fluidization and mixing of the particles. The particle volume fraction is hence comparatively steady and does not change appreciably over time. On the other hand, the gas is evenly dispersed at the bottom of the reactor in the reactor with a distributor plate. This causes the fluidization and mixing of the particles inside the reactor to be more consistent. Particle volume fraction fluctuates highly resulted from this.

6.2.5 Comparison through hot bed model

Figure 6.12 shows the results comparison of syn gas production from experiments of the reactor with two sides nozzles gasifier located in USN, simulations through the nozzle, and uniform distribution in hot bed conditions. From the figure, the results of the simulation of two side nozzles are close to the experimental value deviated by 10.4%. From the figure, the production of methane and carbon monoxide gas is high in the reactor with uniform distribution compared to experimental value and simulation through the reactor of side nozzles whereas methane production was almost the same for experimental value and reactor with nozzle, but carbon monoxide production is less than experimental value for nozzle diameter simulation. Production of carbon dioxide gas was higher in the experimental and reactor with nozzles than reactor with uniform distribution. And the production of hydrogen was almost the same between the uniform distribution and experiments but a bit less in the reactor with side nozzles. But in case of Nitrogen gas, it has high mole fraction in product gas more than a bit more in the nozzle type reactor and less in the uniform distribution reactor which was less than 50. Overall, syn gas production was seen high in the reactor with uniform distribution, then nozzles simulations were higher by 8.33% by mole of the fraction.

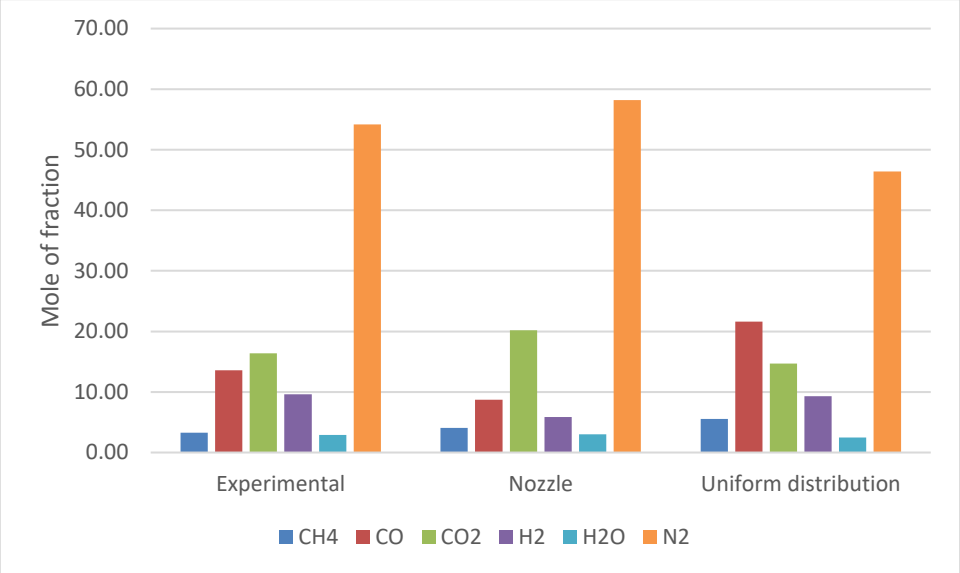

Figure 6.12 Comparison of results of hot bed model between experiment and simulation

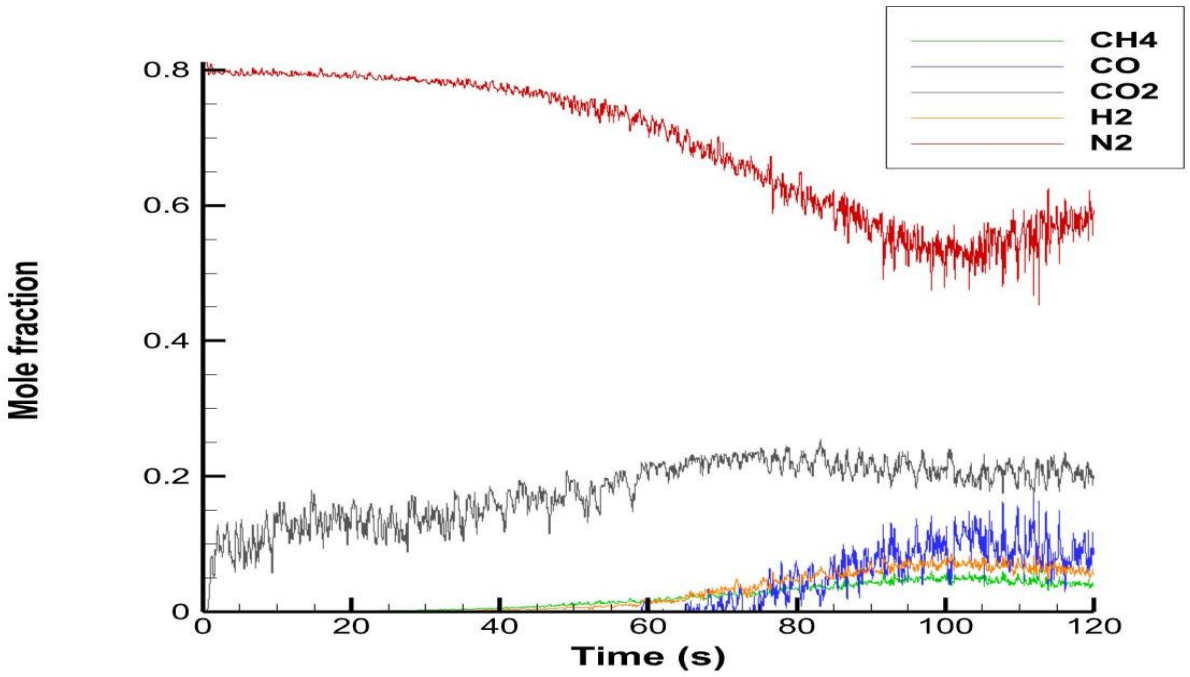

Figure 6.13 Mole fractions of Product gases at different time steps in nozzle type reactor

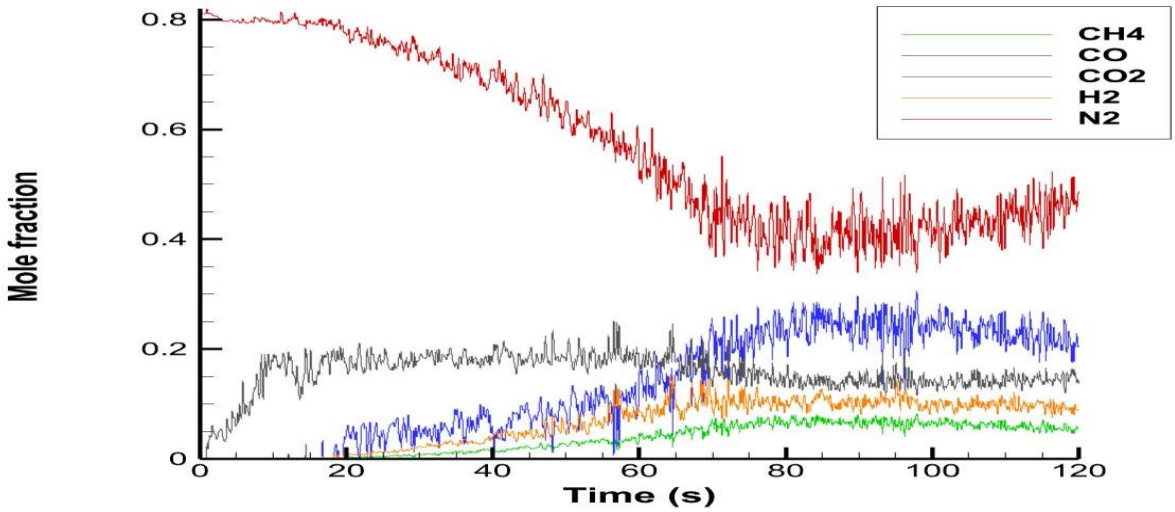

Figure 6.14 Mole fractions of Product gases at different time steps in uniform distribution type reactor

In Figures 6.13 and 6.14, the chemical composition of product gases is shown at different time steps for the reactor with nozzles and the reactor with uniform distribution, respectively. In Figure 6.13 carbon dioxide seems to form at the start of the simulation in both cases whereas other products start to appear after 40-60 seconds time steps in the reactor with nozzle bit in the case of the reactor with uniform distributions other product gases begin to form after 20-30 seconds time steps. It shows that product gases started to form earlier in the reactor with uniform distributions than the nozzle.

Here, maybe the production of syn's just started to see from 60 seconds effectively because in the case of nozzles, most of the bubbles appear in the side of the reactor for a certain time so on increasing with time production goes on increasing as a result flow has been observed all over the reactor but in case of the reactor with uniform distribution flows appear all over the reactor from initially so production of gas seen early. Here I took a time step of 120 seconds only, as it times much time to simulation for a longer time. Up to these results, more syn gas production was seen on the reactor with uniform distribution only.

7 Conclusion

The first task of the thesis was accomplished by the construction of a reactor with two side nozzles as inlet flow boundary conditions. The reactor has a 10 cm diameter. Experiments were done in both reactors with four different mixtures of particles. The first experiment was done with silica sand particles with a size ranging from 850–1000 microns. Then three more experiments were carried out with biomass-to-sand ratios of 5%, 10%, and 15% on both reactors. Then the bed was fluidized at different gas velocities by injecting air through the distributor plate and nozzles. The results were analyzed by comparing reactors based on fluidization velocity, mixing and segregation, and bubble behaviors. Furthermore, a Computational Particle Fluid Dynamics (CPFD) model was developed using Barracuda VR software. To validate the model, different drag models were employed, and the simulation results were compared with experimental data. Among the different drag models, the EMMS-Yang-2004 drag model predicted the best result from experimental data. This model was used for further simulations.

The research shows that the minimum fluidization velocity is reduced when biomass particles (Geldart D) are added to sand (Geldart B) in a fluidized bed reactor. The minimum fluidization velocity of sand only of the reactor with side nozzle was obtained at 0.25 m/s and 0.36 m/s for the reactor with distributor plate. This indicates that the reactor with a distributor plate has a higher minimum fluidization velocity than the reactor with side nozzles. Biomass and sand particles mixed better near the minimum fluidization velocity. Along with that, good mixing range of biomass and sand particles were seen at lower biomass percentages.

In the simulation, the results show that the reactor with side nozzles created larger bubbles that emerged from the nozzles and reached the bed's surface mostly rising from the sides of the reactor, whereas the reactor with a uniform distribution produced smaller, more numerous bubbles that were dispersed throughout the bed. Both reactors showed localized segregation, but it was more obvious in the reactor with the uniform distribution. The mixing between biomass and sand particles was visible from the sides of the reactor in the reactor with side nozzles, whereas it occurred throughout the reactor with the reactor with uniform distribution. For the case of particle volume fractions, in the reactor with a uniform distribution, a high fluctuation with time was seen. But in the case of the reactor with side nozzles less fluctuations were seen than the reactor with distributor plate.

References

[1] R. Jaiswal, M. S. Eikeland, B. M. E. Moldestad, and R. K. Thapa, 'Influence on the fluidization pattern of a freely bubbling fluidized bed with different modes of air supply', *Scandinavian Simulation Society*, pp. 291–296, Oct. 2022, doi: 10.3384/ecp192041.

[2] R. Sarker, M. Rahman, N. Love, and A. Choudhuri, 'Effect of Bed Height, Bed Diameter and Particle Shape on Minimum Fluidization in a Gas-Solid Fluidized Bed', presented at the 50th AIAA Aerospace Sciences Meeting Including the New Horizons Forum and Aerospace Exposition, Jan. 2012. doi: 10.2514/6.2012-644.

[3] J. C. Bandara, R. Jaiswal, H. K. Nielsen, B. M. E. Moldestad, and M. S. Eikeland, 'Air gasification of wood chips, wood pellets and grass pellets in a bubbling fluidized bed reactor', *Energy*, vol. 233, p. 121149, Oct. 2021, doi: 10.1016/j.energy.2021.121149.

[4] R. Jaiswal, N. C. I. S. Furuvik, R. K. Thapa, and B. M. E. Moldestad, 'A CPFD model to investigate the influence of feeding positions in a gasification reactor', *Int. J. EQ*, vol. 5, no. 3, pp. 223–233, Sep. 2020, doi: 10.2495/EQ-V5-N3-223-233.

[5] P. Basu, 'Combustion and Gasification in Fluidized Beds', *Combustion and Gasification in Fluidized Beds*, p. 77, 2006, Accessed: Jan. 09, 2023. [Online]. Available: https://www.academia.edu/10784958/Combustion_and_Gasification_in_Fluidized_Beds

[6] '341355.pdf'. Accessed: Jan. 16, 2023. [Online]. Available: https://discovery.ucl.ac.uk/id/eprint/1349342/1/341355.pdf

[7] R. Jaiswal, 'Computational modeling and experimental studies on fluidized bed regimes'.

[8] C. A. S. Felipe and S. C. S. Rocha, 'Time series analysis of pressure fluctuation in gas-solid fluidized beds', *Braz. J. Chem. Eng.*, vol. 21, pp. 497–507, Sep. 2004, doi: 10.1590/S0104-66322004000300014.

[9] C. E. Agu, 'Bubbling Fluidized Bed Behaviour for Biomass Gasification', Doctoral thesis, University of South-Eastern Norway, 2019. Accessed: Apr. 19, 2023. [Online]. Available: https://openarchive.usn.no/usn-xmlui/handle/11250/2618843

[10] D. Kunii and O. Levenspiel, *Fluidization Engineering*. Butterworth-Heinemann, 1991.

[11] C. Dechsiri, 'Particle Transport in Fluidized Beds: Experiments and Stochastic Models', Thesis fully internal (DIV), s.n., Groningen, 2004.

[12] *Fluidization Engineering by D. Kunii, Octave Levenspiel - Ebook | Scribd*. Accessed: Apr. 28, 2023. [Online]. Available: https://www.scribd.com/book/282479383/Fluidization-Engineering

[13] 'Mc.Cabe-WL-Smith-JC-and-Harriott-P_Unit-operation-of-chemical-engineering.pdf'. Accessed: Apr. 19, 2023. [Online]. Available: https://foodtechnotes.com/wp-content/uploads/2020/05/Mc.Cabe-WL-Smith-JC-and-Harriott-P_Unit-operation-of-chemical-engineering.pdf

[14] S. Ergun and A. A. Orning, 'Fluid Flow through Randomly Packed Columns and Fluidized Beds', *Ind. Eng. Chem.*, vol. 41, no. 6, pp. 1179–1184, Jun. 1949, doi: 10.1021/ie50474a011.

[15] Y. Yang *et al.*, 'Monitoring of particle motions in gas-solid fluidized beds by electrostatic sensors', *Powder Technology*, vol. 308, pp. 461–471, Feb. 2017, doi: 10.1016/j.powtec.2016.11.034.

[16] G. Emig, W. Bauer, and H. J. Werther, 'Influence of gas distributor design on the performance of fluidized bed reactor', *Ger. Chem. Eng. (Engl. Transl.); (Germany, Federal Republic of)*, vol. 4:5, Oct. 1981, Accessed: Apr. 19, 2023. [Online]. Available: https://www.osti.gov/etdeweb/biblio/6771154

[17] J. Davidson, 'The Dynamics of Fluidized Particles. By R. JACKSON, Cambridge University Press, 2000. 339 pp. ISBN 0521781221. £42.50', *Journal of Fluid Mechanics*, vol. 433, pp. 410–412, Apr. 2001, doi: 10.1017/S0022112001003834.

[18] E. R. Gilliland, 'Fluidised particles, J. F. Davidson and D. Harrison, Cambridge University Press, New York (1963). 155 pages. $6.50', *AIChE Journal*, vol. 10, no. 5, pp. 783–785, 1964, doi: 10.1002/aic.690100503.

[19] P. Salatino and R. Solimene, 'Mixing and segregation in fluidized bed thermochemical conversion of biomass', *Powder Technology*, vol. 316, pp. 29–40, Jul. 2017, doi: 10.1016/j.powtec.2016.11.058.

[20] T. Emiola-Sadiq, J. Wang, L. Zhang, and A. Dalai, 'Mixing and segregation of binary mixtures of biomass and silica sand in a fluidized bed', *Particuology*, vol. 58, pp. 58–73, Oct. 2021, doi: 10.1016/j.partic.2021.01.010.

[21] M. Syamlal and T. O'Brien, 'Computer simulation of bubbles in a fluidized bed', *AIChE Symposium Series*, vol. 85, pp. 22–31, Jan. 1989.

[22] S. Chiba, T. Chiba, A. W. Nienow, and H. Kobayashi, 'The minimum fluidisation velocity, bed expansion and pressure-drop profile of binary particle mixtures', *Powder Technology*, vol. 22, no. 2, pp. 255–269, Mar. 1979, doi: 10.1016/0032-5910(79)80031-5.

[23] J. Tang, X. Chen, C. Lu, and Y. Zhang, 'Minimum Fluidization Velocity of Binary Particles with Different Geldart Classification', *Advanced Materials Research*, vol. 482–484, pp. 655–662, Feb. 2012, doi: 10.4028/www.scientific.net/AMR.482-484.655.

[24] D. Mehta and M. C. Hawley, 'Wall Effect in Packed Columns', *Ind. Eng. Chem. Proc. Des. Dev.*, vol. 8, no. 2, pp. 280–282, Apr. 1969, doi: 10.1021/i260030a021.

[25] W. Amarasinghe, C. Jayarathna, B. Ahangama, B. Moldestad, and L.-A. Tokheim, 'Experimental Study and CFD Modelling of Minimum Fluidization Velocity for Geldart A, B and D Particles', *International Journal of Modeling and Optimization*, vol. 7, pp. 152–156, Jun. 2017, doi: 10.7763/IJMO.2017.V7.575.

[26] A. Reyes-Urrutia, J. P. Capossio, C. Venier, E. Torres, R. Rodriguez, and G. Mazza, 'Artificial Neural Network Prediction of Minimum Fluidization Velocity for Mixtures of Biomass and Inert Solid Particles', *Fluids*, vol. 8, no. 4, Art. no. 4, Apr. 2023, doi: 10.3390/fluids8040128.

[27] K. Noda, S. Uchida, T. Makino, and H. Kamo, 'Minimum fluidization velocity of binary mixture of particles with large size ratio', *Powder Technology*, vol. 46, no. 2, pp. 149–154, Apr. 1986, doi: 10.1016/0032-5910(86)80021-3.

[28] A. W. Nienow, P. N. Rowe, and L. Y.-L. Cheung, 'A quantitative analysis of the mixing of two segregating powders of different density in a gas-fluidised bed', *Powder Technology*, vol. 20, no. 1, pp. 89–97, May 1978, doi: 10.1016/0032-5910(78)80013-8.

[29] T. Helmer Pedersen and F. Conti, ‘Improving the circular economy via hydrothermal processing of high-density waste plastics’, *Waste Management*, vol. 68, pp. 24–31, Oct. 2017, doi: 10.1016/j.wasman.2017.06.002.

[30] M. Stein, Y. L. Ding, J. P. K. Seville, and D. J. Parker, ‘Solids motion in bubbling gas #uidised beds’, *Chemical Engineering Science*, 2000.

[31] J. A. Laverman *et al.*, ‘Experimental study on the influence of bed material on the scaling of solids circulation patterns in 3D bubbling gas–solid fluidized beds of glass and polyethylene using positron emission particle tracking’, *Powder Technology*, vol. 224, pp. 297–305, Jul. 2012, doi: 10.1016/j.powtec.2012.03.011.

[32] Y. Li, H. Fan, and X. Fan, ‘Identify of flow patterns in bubbling fluidization’, *Chemical Engineering Science*, vol. 117, pp. 455–464, Sep. 2014, doi: 10.1016/j.ces.2014.07.012.

[33] C. Agu and B. M. E. Moldestad, ‘Distribution of Solids in a Fluidized Bed Operated without a Gas Distributor’, presented at the The 59th Conference on imulation and Modelling (SIMS 59), 26-28 September 2018, Oslo Metropolitan University, Norway, Nov. 2018, pp. 248–254. doi: 10.3384/ecp18153248.

[34] ‘Fluctuations and waves in fluidized bed systems--The influence of the air-supply system - 百度文库’. https://wenku.baidu.com/view/5c847f80102de2bd97058818.html?_wkts_=1682337760153 (accessed Apr. 24, 2023).

[35] J. C. Bandara, H. K. Nielsen, B. M. E. Moldestad, and M. S. Eikeland, ‘Sensitivity Analysis and Effect of Simulation parameters of CPFD Simulation in Fluidized Beds’, presented at the The 59th Conference on imulation and Modelling (SIMS 59), 26-28 September 2018, Oslo Metropolitan University, Norway, Nov. 2018, pp. 334–341. doi: 10.3384/ecp18153334.

[36] H. K. Versteeg and W. Malalasekera, *An introduction to computational fluid dynamics: the finite volume method*, 2nd ed. Harlow, England ; New York: Pearson Education Ltd, 2007.

[37] S. Teng, C. Kang, K. Ding, C. Li, and S. Zhang, ‘CFD-DEM Simulation of the Transport of Manganese Nodules in a Vertical Pipe’, *Applied Sciences*, vol. 12, no. 9, Art. no. 9, Jan. 2022, doi: 10.3390/app12094383.

[38] A. Abbasi, P. E. Ege, and H. I. De Lasa, ‘CPFD simulation of a fast fluidized bed steam coal gasifier feeding section’, *Chemical Engineering Journal*, vol. 174, no. 1, pp. 341–350, Oct. 2011, doi: 10.1016/j.cej.2011.07.085.

[39] A. Shynybayeva and L. Rojas-Solórzano, ‘Eulerian-Eulerian Modeling of Multiphase Flow in Horizontal Annuli: Current Limitations and Challenges’, *Processes*, vol. 8, pp. 1-24 (1426), Nov. 2020, doi: 10.3390/pr8111426.

[40] A. Schröder and D. Schanz, ‘3D Lagrangian Particle Tracking in Fluid Mechanics’, *Annual Review of Fluid Mechanics*, vol. 55, no. 1, pp. 511–540, 2023, doi: 10.1146/annurev-fluid-031822-041721.

[41] D. M. Snider, ‘An Incompressible Three-Dimensional Multiphase Particle-in-Cell Model for Dense Particle Flows’, *Journal of Computational Physics*, vol. 170, no. 2, pp. 523–549, Jul. 2001, doi: 10.1006/jcph.2001.6747.

[42] Q. Wang *et al.*, ‘Application of CPFD method in the simulation of a circulating fluidized bed with a loop seal, part I—Determination of modeling parameters’, *Powder Technology*, vol. 253, pp. 814–821, Feb. 2014, doi: 10.1016/j.powtec.2013.11.041.

[43] W. K. Ariyaratne, E. V. P. J. Manjula, C. Ratnayake, and M. Melaaen, ‘CFD Approaches for Modeling Gas-Solids Multiphase Flows – A Review’, Sep. 2016. doi: 10.3384/ecp17142680.

[44] J. I. Okoro, ‘Development of a CPFD model-based technique to optimize feed pellets transfer systems in fish farms’.

[45] E. Zhang, X. Lan, and J. Gao, ‘Modeling of gas-solid flow in a CFB riser based on computational particle fluid dynamics’, *Petroleum Science*, vol. 9, Dec. 2012, doi: 10.1007/s12182-012-0240-7.

[46] V. Verma and J. T. Padding, ‘A novel approach to MP-PIC: Continuum particle model for dense particle flows in fluidized beds’, *Chemical Engineering Science: X*, vol. 6, p. 100053, Feb. 2020, doi: 10.1016/j.cesx.2019.100053.

[47] F. A. Williams, *Combustion Theory*, 2nd ed. Boca Raton: CRC Press, 2019. doi: 10.1201/9780429494055.

Appendices

Appendix A
Sign Task Description

University of South-Eastern Norway

Faculty of Technology, Natural Sciences and Maritime Sciences, Campus Porsgrunn

FMH606 Master's Thesis

Title: Design and construction of a bubbling fluidized bed reactor with two side nozzles as inlet flow boundary conditions

USN supervisors: Rajan Thapa, Rajan Jaiswal (co-supervisor)

Task background:

Fluidized bed reactors are widely used for several industrial applications like waste to energy conversion, chemical synthesis, granulation, drying of pharmaceutical products and raw agricultural products, chemical looping, catalyst regeneration, biomass gasification, pyrolysis etc. Recently, the fluidized bed has gained popularity due to its advantageous properties like uniform heat and mass transfer, better temperature control, and good mixing. The efficiency of the fluidized bed reactors largely depends on the gas distribution inside the reactor since the gas distribution influences the conversion process and the fluidization regime under which the reactor is operated. For instance, during the gasification of biomass or wastes using a bubbling fluidized bed reactor, the carbanions feedstock is converted into higher calorific value gases in the presence of a limited amount of oxidizing agent. The amount of oxidizing medium present for the feedstock conversion depends on how well the fluidizing gas is distributed across the reactor cross-section. Similarly, the hot bed material which acts as a thermal flywheel is set into continuous motion by supplying fluidizing gas through the particle bed. Additionally, the mixing phenomena of large biomass particles with bed material are determined by the fluidizing gas to the reactor.

The fluidizing gas can be supplied to the particle bed through the air distributor or nozzles. The most common method has been the use of a distributor plate. However, the use of an air distributor plate increases the auxiliary power consumption required to pump the gas through the reactor. Additionally, the distributor plate has to be selected depending on the reactor types and process as the distributor plays a critical role in the reactor performance. In addition, there are challenges in operating the reactor with the distributor plate, which requires regular cleaning and maintenance due to the clogging of the pores of the distributor plate by the fine particles and sintering. Alternatively, a nozzle can be employed to fluidize the particle bed which can overcome the challenges associated with air distribution. There is not much research on this topic.

This research work will focus on the modification of a bubbling fluidized bed reactor located at USN. Two side nozzles will be added to the reactor as air supply boundary conditions. A series of experiments will be conducted on the rig with a binary mixture of Geldart B and Geldar D particles to characterize the fluid dynamics behaviour of the reactor. Additionally, a CPFD model in Barracuda VR will be used to predict the flow behaviour of the hot bed conditions with side nozzles as flow boundary conditions.

Task description:

Objectives:

The major objectives of this project work are:

1. To construct and develop a cold model of a bubbling fluidized bed reactor withtwo side nozzles for the fluidizing gas inlet.
2. Develop a CPFD model to predict the flow behaviour of a binary mixture of Geldart D and Geldart B particles in a bubbling fluidized bed reactor with sidenozzles as gas inlet flow boundary conditions.

To accomplish the objectives following experimental and simulation tasks will be carried out:

Experimental tasks:

- Construction of a reactor with two side nozzles as an inlet for fluidizing gassupply.
- Carry out experiments on a newly modified bubbling fluidized bed reactor.
- Characterization of the fluidizing behaviour (minimum fluidization, mixing andsegregation) of Geldart D and Geldart B particles from the experimental data.
- Compare the experimental data measured from the modified reactor with theexperimental data obtained from the reactor with the air distributor.

Simulation tasks:

- Develop a CPFD model of the reactor and validate it with experimental data.
- Simulate hot bed conditions and compare the simulation results with theexperimental data obtained from the gasifier at USN.

Student category: Reserved for Suraj Shrestha

The task is suitable for online students (not present at the campus): No

Practical arrangements:
Experimental works will be carried out at the 20 kW gasification reactor and a cold flow model located at USN, Porsgrunn Campus. A CPFD simulation software barracuda will beavailable for a certain period.

Supervision:
As a general rule, the student is entitled to 15-20 hours of supervision. This includes the necessary time for the supervisor to prepare for supervision meetings (reading material tobe discussed, etc).

Signatures:
Supervisor (date and signature): 

Student (write clearly in all capitalized letters): SURAJ SHRESTHA

Student (date and signature): 2023-05-12 surajstha

Appendix B

Pressure drops per length vs superficial gas velocity data of reactor with nozzle and reactor with distributor plate

Superficial velocity(m/s)	Pressure drops (P) (Reactor with nozzle)	Pressure drops (P) (Reactor With distributor plate)
0.13	5976.15	2226.27
0.15	6984.91	3114.14
0.17	8176.13	4060.46
0.19	9407.53	5074.96
0.21	10647.29	6050.50
0.23	12672.96	7194.58
0.25	14062.96	8124.03
0.28	13179.72	9209.61
0.30	13458.83	10468.95
0.32	12127.79	11260.03
0.34	12611.13	11940.03
0.36	12298.82	12337.41
0.38	11431.93	11604.97
0.40	11377.41	11236.24
0.42	11138.52	10747.84
0.45	10813.98	10549.98
0.47	11244.23	10798.65
0.49	10756.89	10289.78
0.51	10889.19	10290.61
0.53	10336.70	10036.02
0.55	10780.28	10186.29
0.57	10055.68	10016.56
0.59	10379.26	10809.15
0.62	10255.12	9763.10
0.64	10312.20	9977.26

Appendix C

Model Validation Data

Superficial velocity(m/s)	Pressure drops per unit length (Pascal) (Experiment)	Pressure drops per unit length (Pascal) (Simulations)
0.085	3871.31	4332.62
0.106	4918.54	6002.7
0.127	5976.15	7120.74
0.148	6984.91	8234.54
0.17	8176.13	9354.47
0.191	9407.53	10397.22
0.202	9579.7	11440.27
0.212	10647.29	11949.08
0.233	12672.19	12320.56
0.244	13762.96	13569.63
0.255	14156.92	14644.89
0.265	13212.34	13401.01
0.276	13179.72	13960.86
0.286	13103.74	12736.4
0.297	13458.83	12298.08
0.308	13252.48	12266.2
0.318	12981.82	12243.46
0.339	12611.13	12349.56
0.361	12298.82	12338.69
0.382	11431.93	12540.34
0.403	11377.41	12584.55
0.424	11138.52	12765.23
0.445	10813.98	12688.18
0.467	11244.23	12197.18

Appendix D

Mole fractions of products

Mole fractions	Experimental	Simulation (reactor with nozzle)	Simulation (reactor with Uniform distribution)
CH4	3.28	4.07	5.56
CO	13.59	8.70	21.6
CO2	16.37	20.20	14.7
H2	9.60	5.84	9.31
H2O	2.90	3.01	2.5
N2	54.15	58.20	46.4